

Deepfake Generation and Detection: A Benchmark and Survey

Gan Pei*, Jiangning Zhang*†, Menghan Hu†, Zhenyu Zhang, Chengjie Wang, Yunsheng Wu,
Guangtao Zhai, Jian Yang, Chunhua Shen, Dacheng Tao

Abstract—Deepfake is a technology dedicated to creating highly realistic facial images and videos under specific conditions, which has significant application potential in fields such as entertainment, movie production, digital human creation, to name a few. With the advancements in deep learning, techniques primarily represented by Variational Autoencoders and Generative Adversarial Networks have achieved impressive generation results. More recently, the emergence of diffusion models with powerful generation capabilities has sparked a renewed wave of research. In addition to deepfake generation, corresponding detection technologies continuously evolve to regulate the potential misuse of deepfakes, such as for privacy invasion and phishing attacks. This survey comprehensively reviews the latest developments in deepfake generation and detection, summarizing and analyzing current state-of-the-arts in this rapidly evolving field. We first unify task definitions, comprehensively introduce datasets and metrics, and discuss developing technologies. Then, we discuss the development of several related sub-fields and focus on researching four representative deepfake fields: face swapping, face reenactment, talking face generation, and facial attribute editing, as well as forgery detection. Subsequently, we comprehensively benchmark representative methods on popular datasets for each field, fully evaluating the latest and influential published works. Finally, we analyze challenges and future research directions of the discussed fields.

Index Terms—Deepfake Generation, Face Swapping, Face Reenactment, Talking Face Generation, Facial Attribute Editing, Forgery detection, Survey

1 INTRODUCTION

ARTIFICIAL Intelligence Generated Content (AIGC) has garnered considerable attention [1] in academia and industry in recent years. Deepfake generation, as one of the important technologies in the generative domain, has gained significant attention due to its ability to create highly realistic facial media content. This technique has undergone a transition from traditional graphics-based methods to deep learning-based approaches. Early methods employed advanced Variational Autoencoder [2], [3], [4] (VAEs) and Generative Adversarial Networks [5], [6] (GANs) techniques, enabling seemingly realistic image generation, but its performance is still unsatisfactory that limits practical applications. Recently, the Diffusion [7], [8], [9] structure has greatly enhanced the generation capability of images/videos. Benefiting from this new wave of research, the deepfake technology allows us to see the potential values for the practical application, and it can generate indistinguishable contents against real ones, which has further attracted our attention

and is widely applied in numerous fields [10], including entertainment, movie production, online live broadcasting, virtual meetings, new insights for privacy protection, etc.

Deepfake generation can generally be divided into four mainstream research fields: 1) Face swapping [11], [12], [13] is dedicated to executing identity exchanges between two person images; 2) Face reenactment [14], [15], [16] emphasizes transferring source movements and poses; 3) Talking face generation [17], [18], [19] focuses on achieving natural matching of mouth movements to textual content in character generation, and 4) Facial attribute editing [20], [21], [22] aims to modify specific facial attributes of the target image. The development of related foundational technologies has gradually shifted from single forward GAN models [5], [23] to multi-step diffusion models [7], [24], [25] with higher quality generation capabilities, and the generated content has also gradually transitioned from single-frame images to temporal video modeling [8]. In addition, NeRF [26], [27] has been frequently incorporated into modeling to improve multi-view consistency capabilities [28], [29].

While enjoying the novelty and convenience of this technology, the unethical use of it raises concerns over the spread of privacy invasion, and dissemination of fake news, necessitating the development of effective forgery detection methods [30] in opposition, *a.k.a.*, deepfake detection. From the earliest handcrafted feature-based methods [31], [32] to deep learning-based methods [33], [34], and the recent hybrid detection techniques [35], forgery detection has undergone substantial technological advancements along with the development of generative technologies. The data modality has also transitioned from the spatial and frequent domains [36], [37] to the more challenging temporal domain [38], [39].

- G. Pei and M. Hu are with the Shanghai Key Laboratory of Multidimensional Information Processing, School of Communication and Electronic Engineering, East China Normal University, Shanghai, 200241, China.
- J. Zhang, C. Wang, and Y. Wu are with YouTu Lab, Tencent, China.
- Z. Zhang and J. Yang are with School of Intelligence Science and Technology, Nanjing University, China.
- G. Zhai is with the Institute of Image Communication and Network Engineering, Shanghai Jiao Tong University Shanghai, 200240, China.
- C. Shen is with Zhejiang University, China.
- D. Tao is with Singapore Management University, Singapore.
- Gan Pei and Jiangning Zhang contribute equally.
- Corresponding authors[†]: Menghan Hu and Jiangning Zhang.
- We closely follow the latest developments in this *project*.

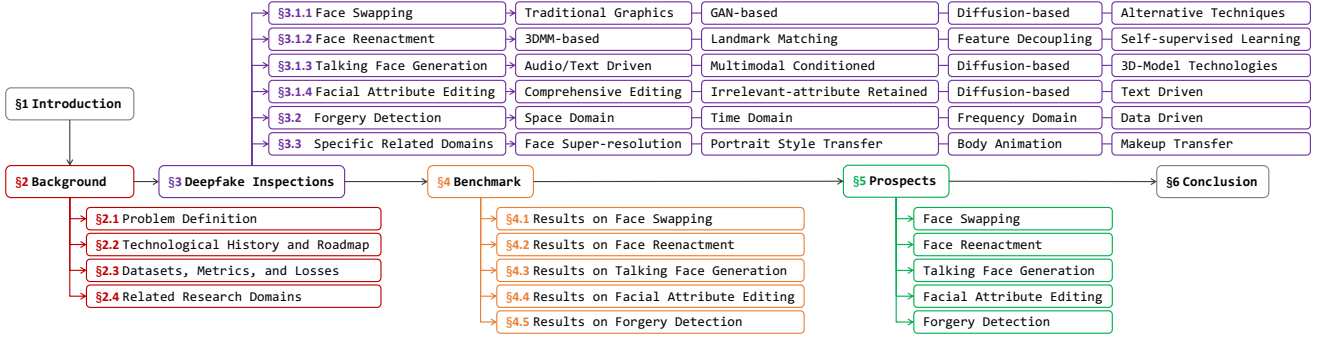


Fig. 1: Time diagram that reflects the survey pipeline. Zoom in for a better holistic perception of this work.

Considering that current generative technologies have a higher level of interest, develop faster, and can generate indistinguishable content from reality [40], corresponding detection technologies need continuous evolution.

Overall, despite the significant progress made in both directions, they still exhibit challenging limitations in specific scenarios [41], mainly reflected in the visual perception authenticity and generative accuracy of models. This has attracted a large number of researchers to continue their efforts and has sparked thoughts on industrial applications. Existing survey works only focus on partial deepfake fields and lack discussions on new technologies [1], [40], [42], especially diffusion-based image/video generation methods, due to their disconnection from current technologies. The survey will comprehensively discuss these fields as well as related sub-fields, and cover tracking of the latest works.

- **Contribution.** In this survey, we comprehensively explore the key technologies and latest advancements in Deepfakes generation and forgery detection. We first unify the task definitions (Sec. 2.1), provide a comprehensive comparison of datasets and metrics (Sec. 2.3), and discuss the development of related technologies. Specifically, we investigate four mainstream deepfake fields: face swapping (Sec. 3.1.1), face reenactment (Sec. 3.1.2), talking face generation (Sec. 3.1.3), and facial attribute editing (mainly on multiple editing) (Sec. 3.1.4), as well as forgery detection (Sec. 3.2). We also analyze the benchmarks and settings for each domain, thoroughly evaluating the latest and influential works published in top-tier conferences/journals (Sec. 4), especially recent diffusion-based approaches. Additionally, we discuss closely related fields, including head swapping, face super-resolution, face reconstruction, face inpainting, body animation, portrait style transfer, makeup transfer, and adversarial sample detection. Benefiting from the current popularity of AIGC, the research iteration cycle in the deepfake field has been significantly reduced, and we keep updating and discussing the in-submission works in the revised version.

- **Scope.** This survey primarily focuses on mainstream face-related tasks, including face swapping, face reenactment, talking face generation, facial (multiple) attribute editing, and forgery detection. We also cover some related domain tasks in Sec. 2.4 and detail specific popular sub-tasks in Sec. 3.3. Considering the large number of articles (including published and preprints), we mainly include representative and attention-grabbing works. In addition, we compare this investigation with recent surveys. Sha *et al.* [1] only discuss character generation while we cover a more comprehensive

range of tasks. Compared to works [40], [42], [43], our study encompasses a broader range of technical models, particularly the more powerful diffusion-based methods. Additionally, we thoroughly discuss the related sub-fields of deepfake generation and detection.

- **Survey Pipeline.** Fig. 1 shows the pipeline of this survey. Sec. 2 provides the essential background knowledge that encompasses task-specific definitions, datasets, evaluation metrics, and exploration of related research areas. Sec. 3 presents technical discussions, examining four most popular deepfake tasks from the perspective of technological categorization and evolution. In addition, we meticulously classify and discuss forgery detection techniques, emphasizing the technological routes involved. Subsequently, Sec. 4 organizes and evaluates performance from various approaches for a thorough and fair performance comparison. Sec. 5 focuses on a critical review of the challenges that persist in existing techniques, outlining feasible future development directions. Finally, we encapsulate the entirety of the paper through a comprehensive summary in Sec. 6.

2 BACKGROUND

In this section, we first introduce the conceptual definitions of the discussed mainstream fields. Fig. 2 illustrates intuitive objectives for each task and shows the distinctions among tasks in terms of manipulated facial components. Then, we review the developmental history of commonly used neural networks, highlighting several representative ones. Next, we summarize popular datasets, metrics, and loss functions. Finally, we comprehensively discuss several relevant domains.

2.1 Problem Definition

- **Unified Formulation of Studied Problems.** Fig. 2 intuitively displays the various deepfakes generation and detection tasks studied in this paper. For the former, different tasks can essentially be expressed as controlled content generation problems under specific conditions, such as images, audio, text, specific attributes, *etc.*. Given the target image I_t to be manipulated and the condition information $C = \{\text{Image}, \text{Audio}, \text{Text}, \dots\}$, the content generation process can be represented as:

$$I_o = \phi_G(I_t, C), \quad (1)$$

where ϕ_G abstracts the specific generation network and $I_o = \{I_t^0, I_t^1, \dots, I_t^{N-1}\}$ represents generated contents. N is the total frame number for the generated video, which is set to 1

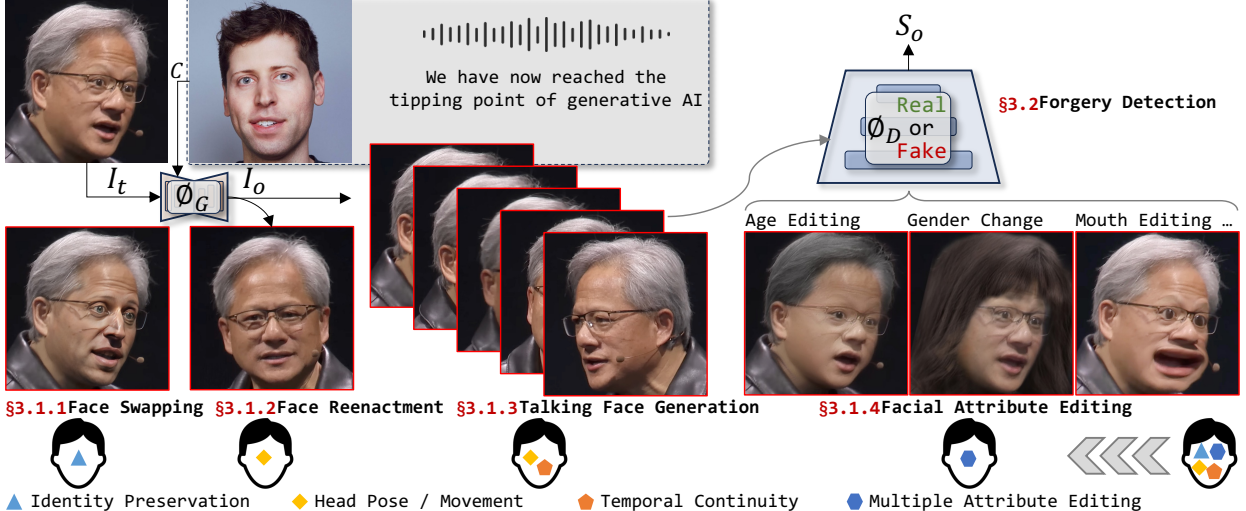


Fig. 2: Top: Illustration of different deepfake generation (Sec. 3.1) and detection (Sec. 3.2) tasks that are discussed in this survey. Bottom: Specific facial attribute modification of each task. Data from [NVIDIA Keynote at COMPUTEX 2023](#) at 29:40.

by default). The latter task can be viewed as an image-level or pixel-level classification problem as practical application needs, which can be represented as:

$$S_o = \phi_D(I_o), \quad (2)$$

where ϕ_D abstracts the specific detection network and S_o represents the fake score for the generated content I_o .

- **Face Swapping** involves replacing the identity information of the target face I_t by the source face $C=I_s$, while preserving ID-irrelevant attributes of the target face, such as skin color and expressions.

- **Face Reenactment** alters the facial movement of a target image I_t without changing the identity and other facial attributes, under the conditions of driving image, video, head pose, etc.. This technology often involves the support of facial motion capture technology, such as facial tracking or prediction based on deep learning models [44].

- **Talking Face Generation** can be viewed as an extension in time, aiming at generating a talking video $I_o=\{I_o^i\}$, $i=0, 1, \dots, N-1$ with the character in the target image I_t engaging in a conversation based on an arbitrary driving source, such as text, audio, video, or a multi-modal composite source. The lip movements, facial poses, expressions, emotions, and spoken content information of the character in the generated video match the target information.

- **Facial Attribute Editing** aims to modify the semantic information of the target face I_t (e.g., personality, age, expressions, skin color, etc.) in a directed manner based on individual interest and preference. Existing methods include single and comprehensive attribute editing: the former focuses on training a model for only one attribute, while the latter integrates multiple attribute editing tasks simultaneously that is our primary focus in this survey.

- **Forgery Detection** aims to detect and identify anomalies, tampering, or forgery areas in images or videos by the anomaly score S_o , and it has great research and application value in information security and multimedia forensics.

2.2 Technological History and Roadmap

- **Generative Framework.** Variational Autoencoders (VAEs) [2], [3], [4], Generative Adversarial Networks (GANs) [5], [6], [23], and Diffusion [24], [25], [45] have played pivotal roles in the developmental history of generative models. 1) VAE [2] emerged in 2013, altering the relationship between latent features and linear mappings in autoencoder latent spaces. They introduced feature distributions like the Gaussian distribution and achieved the generation of new entities through interpolation. To enhance generation capabilities under specific conditions, CVAE [3] introduced conditional input. VQ-VAE [4] introduced the concept of Vector Quantization to improve the learning of latent representations. Subsequent models are continually advancing. 2) GANs [23] achieves high-quality generation through the adversarial training with an extra discriminator. Subsequently, research on GANs experienced a surge, and currently, the implementation based on GANs remains the mainstream approach for various deepfake tasks. CGAN [46] introduced conditional control variables to GANs. Pix2Pix [47] enhanced GAN performance in specific image translation tasks. StyleGAN [5] introduced the concept of style transfer to GANs. StyleGAN2 [6] further improved the quality and controllability of generated images. Additionally, some composite research combines GANs with VAE, e.g. CVAE-GAN [48]. 3) Diffusion modal [45] models the generation of data as a diffusion process. DDPM [24] gains widespread attention for its outstanding generative performance, especially when the model excels in handling large-scale, high-resolution images. LDM [25] is more flexible and powerful when it comes to modeling complex data distributions. In the field of video generation, Diffusion models play a crucial role [49], [50]. SVD [7] fine-tunes the base model using an image-to-video conversion task based on text-to-video models. AnimateDiff [8] attaches a newly initialized motion modeling module to a frozen text-to-image model and trains it in subsequent video clips to refine reasonable motion prior knowledge, thus achieving excellent generation results.

- **Discriminative Neural Network.** Convolutional Neural Networks (CNNs) [51], [52], [53], [54], [55], [56] have played



Fig. 3: Development timeline of three mainstream generative models, *i.e.*, **VAE**, **GAN**, and **Diffusion**.

a pivotal role in the history of deep learning. LeNet [51], as the pioneer of CNNs, showcased the charm of machine learning. AlexNet [52] and ResNet [53] made deep learning feasible. Recently, ConvNeXt [54] has achieved excellent results surpassing those of Swin-Transformer [57]. The Transformer architecture initially proposed [58] in 2017. The core idea involves using self-attention mechanisms to capture dependencies between different positions in the input sequence, enabling global modeling of sequences. ViT [59] demonstrates that using Transformer in the field of computer vision can still achieve excellent performance and PVT [60] overcomes the challenges of adapting Transformer to various dense prediction tasks. In addition, Swin-Transformer [57] addresses the limitations of Transformer in handling high-resolution image processing tasks. Subsequently, Swin-Transformer V2 [61] further improves the model's efficiency and the resolution of manageable inputs.

- **Neural Radiance Field** (NeRF) is first introduced in 2020 [26], with its core idea revolving around the use of volume rendering and implicit neural fields to represent and reconstruct both geometric and illumination information of 3D scenes [27]. Compared to traditional 3D methods, it exhibits higher visual quality and is currently widely applied in tasks such as 3D geometry enhancement [62], [63], segmentation [64] and 6D pose estimation [65]. In addition, Some notable works [66], [67] combining NeRF as a supplement to 3D information and generation models are particularly prominent at present.

- **Work Summary.** The evolution of mainstream generative models is depicted chronologically in Fig. 3. This survey delves into four categories of generation tasks along with the forgery detection task, and the publication years distribution of the surveyed articles is shown in Fig. 4.

2.3 Datasets, Metrics, and Losses

- **Dataset.** Given the various datasets in surveyed fields, we use numerical labels to save post-textual space. 1) Commonly used deepfake generation datasets include LFW [68], CelebA [69], CelebA-HQ [72], VGGFace [70], VGGFace2 [73], FFHQ [5], Multi-PIE [85], VoxCeleb1 [71], VoxCeleb2 [74], MEAD [75], MM CelebA-HQ [86], CelebAText-HQ [87], CelebV-HQ [76], TalkingHead-1KH [88], LRS2 [89], LRS3 [90], *etc.* 2) Commonly used forgery detection datasets include UADFV [91], DeepfakeTIMIT [77], FF++ [78], Deepforensics-1.0 [81], DFDCP [79], DFDC [82], CelebDF [83], Celeb-DFv2 [83], FakeAVCeleb [84], DFD [80], WildDeepfake [92], KoDF [93], UADFV [94], Deepfy [95], DF-Platter [96], *etc.* We summarize popular datasets in Tab. 1.

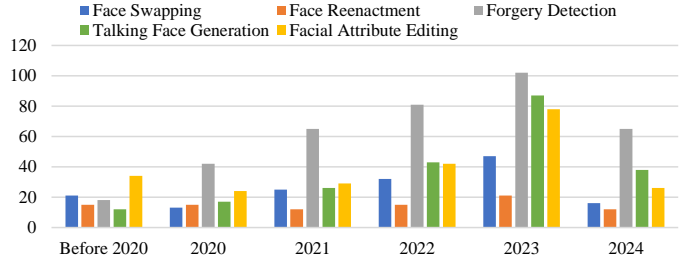


Fig. 4: Works summarization on different directions per year. Data is obtained on 2024/04/20.

- **Metric.** 1) For deepfake generation tasks, commonly used metrics include: Peak Signal-to-Noise Ratio (PSNR) [97], Structured Similarity (SSIM) [98], Learned Perceptual Image Patch Similarity (LPIPS) [99], Fréchet Inception Distance (FID) [100], Kernel Inception Distance (KID) [101], Cosine Similarity (CSIM) [88], Identity Retrieval Rate (ID Ret) [102], Expression Error [103], Pose Error [104], Landmark Distance (LMD) around the mouths [105], Lip-sync Confidence (LSE-C) [106], Lip-sync Distance (LSE-D) [106], *etc.* 2) For forgery generation commonly uses: Area Under the ROC Curve (AUC) [107], Accuracy (ACC) [108], Equal Error Rate (EER) [109], Average Precision (AP) [30], F1-Score [110], *etc.* Detailed definitions are explained in Appendix A.

- **Loss Function.** VAE-based approaches generally employ reconstruction loss and KL divergence loss [2]. Commonly used reconstruction loss functions include Mean Squared Error, Cross-Entropy, LPIPS [99], and perceptual [111] losses. GAN-based methods further introduce adversarial loss [23] to increase image authenticity, while diffusion-based works introduce denoising loss function [24].

2.4 Related Research Domains

- **Head Swapping** replaces the entire head information rather than only the face of the target image [112], including facial contours and hairstyle, with that of the source image. However, in terms of facial attributes, Head Swap only replaces identity attributes, while leaving other attribute information unchanged. Recently, some methods [113], [114] based on Diffusion have been proposed and have shown promising results in achieving good performance.

- **Face Super-resolution** aims to enhance the resolution of low-resolution face images to generate high-resolution face images [115], [116]. This task is closely related to various deepfake sub-tasks. In the early stages of Face Swapping [117], [118] and Talking Face Generation [119], [120], there was consistently a low-resolution issue in the generated images and videos. This problem was addressed by incorporating face super-resolution methods into the models [17], [121] to improve output quality. In terms of technical approaches, FSR can be categorized into methods based on CNNs [122], [123], [124], GANs [125], [126], reinforcement learning [127], and ensemble learning [128].

- **Face Reconstruction** refers to the process of recreating the three-dimensional appearance of an individual's face based on one or multiple 2D facial images [129], [130]. Facial reconstruction often plays an intermediate role in various deepfake sub-tasks. In Face Swapping and Face Reenactment tasks, facial parameters are reconstructed using

TABLE 1: Overview of commonly used datasets. **Orange**-marked ones are selected to evaluate different methods in Sec. 4.

	Dataset	Type	Scale	Highlight
Deepfake Generation	LFW [68]	Image	10K	Facial images captured under various lighting conditions, poses, expressions, and occlusions at 250×250 resolution.
	CelebA [69]	Image	200K	The dataset includes over 200K facial images from more than 10K individuals, each with 40 attribute labels.
	VGGFace [70]	Image	2600K	A super-large-scale facial dataset involving a staggering 26K participants, encompassing a total of 2600K facial images.
	VoxCeleb1 [71]	Video	100K voices	A large scale audio-visual dataset of human speech, the audio includes noisy background interference.
	CelebA-HQ [72]	Image	30K	A high-resolution facial dataset consisting of 30K face images, each with a resolution of 1024×1024 resolution.
	VGGFace2 [73]	Image	3000K	A large-scale facial dataset, expanded with greater diversity in terms of ethnicity and pose compared to VGGFace.
	VoxCeleb2 [74]	Video	2K hours	A dataset that is five times larger in scale than VoxCeleb1 and improves racial diversity.
	FFHQ [5]	Image	70K	The dataset with over 70K high-resolution (1024×1024) facial images, showcasing diverse ethnicity, age, and backgrounds.
Forgery Detection	MEAD [75]	Video	40 hours	An emotional audiovisual dataset provides facial expression information during conversations with various emotional labels.
	CelebV-HQ [76]	Video	35K videos	The dataset's video clips have a resolution of more than 512×512 resolution and are annotated with rich attribute labels.
	DeepfakeTIMIT [77]	Audio-Video	640 videos	The dataset is evenly divided into two versions: LQ (64×64) and HQ (128×128), with all videos using face swapping forgery.
	FF++ [78]	Video	6K videos	Comprising 1K original videos and manipulated videos generated using five different forgery methods.
	DFDCP [79]	Audio-Video	5K videos	The preliminary dataset for The Deepfake Detection Challenge includes two face-swapping methods.
	DFD [80]	Video	3K videos	The dataset comprises 3K deepfake videos generated using five forgery methods.
	Deepforensics [81]	Video	60K videos	The videos feature faces with diverse skin tones, and rich environmental diversity was considered during the filming process.
	DFDC [82]	Audio-Video	128K videos	The official dataset for The Deepfake Detection Challenge and contain a substantial amount of interference information.
FakeAVCeleb [84]	Celeb-DF [83]	Video	1K videos	Comprising 408 genuine videos from diverse age groups, ethnicities, and genders, along with 795 DeepFake videos.
	Celeb-DFv2 [83]	Video	6K videos	An expanded version of Celeb-DFv1, this dataset not only increases in quantity but also the diversity.
	FakeAVCeleb [84]	Audio-Video	20K videos	A novel audio-visual multimodal deepfake detection dataset, deepfake videos generated using four forgery methods.

3DMM, and the model's parameters can be controlled directionally. Additionally, reconstructing a 3D facial model is one of the methods to address the issue of facial artifacts in videos generated under large facial poses. Common technical approaches for facial reconstruction include methods based on 3DMM [131], [132], epipolar geometry [133], one-shot learning [134], [135], shadow shape reconstruction [136], [137], and hybrid learning-based reconstruction [138], [139].

- **Face Inpainting**, *a.k.a.* face completion, aims to reconstruct missing regions in face images caused by external factors such as occlusion and lighting, while preserving facial texture information is crucial in this process [140]. This task is a crucial sub-task of image inpainting, and the current methods are mostly based on deep learning that can be roughly divided into two categories: GAN based [141], [142] and Diffusion based [143], [144].

- **Body Animation** aims to alter the entire bodily pose while unchanging the overall body information [145]. The goal is to achieve a modification of the target image's entire body posture using an optional driving image or video, aligning the body of the target image with the information from the driving signal. The mainstream implementation path for body animation is based on GANs [146], [147], and Diffusion [49], [148], [149], [150].

- **Portrait Style Transfer** aims to reconstruct the style of a target image to match that of a source image by learning the stylistic features of the source image [151], [152]. The goal is to preserve the content information of the target image while adapting its style to that of the source image [153]. Common applications include image cross-domain style transfer, such as transforming real face images into animated face styles [154], [155]. Methods based on GANs [156], [157], [158] and Diffusion [159], [160] have achieved high-quality performance in this task.

- **Makeup Transfer** aims to achieve style transfer learning from a source image to a target image [161], [162]. Existing models have achieved initial success in applying and removing makeup on target images [162], [163], [164], [165], allowing for quantitative control over the intensity of makeup. However, they perform poorly in transferring extreme styles [166], [167], [168]. Existing mainstream methods are based on GANs [161], [169], [170].

- **Adversarial Sample Detection** focuses on identifying whether the input data is an adversarial sample [171]. If

recognized as such, the model can refuse to provide services for it, such as throwing an error or not producing an output [172]. Current deepfake detection models often rely on a single cue from the generation process as the basis for detection, making them vulnerable to specific adversarial samples. Furthermore, relatively little work has focused on adversarial sample testing in terms of model generalization capability and detection evaluation.

3 DEEPFAKE INSPECTIONS: A SURVEY

This section systematically examines four generation tasks: Face Swapping (Sec. 3.1.1), Talking Face Generation (Sec. 3.1.3), Face Reenactment (Sec. 3.1.2), Facial Attribute Editing (Sec. 3.1.4). Additionally, we review techniques for forgery detection (commonly known as deepfake detection) in Sec. 3.2. We document and compare the most representative works in the main text. Furthermore, we discuss several related domains that garnered significant attention in Sec. 3.3.

3.1 Deepfake Generation

3.1.1 Face Swapping

In this section, we review face swapping methods from the perspective of basic architecture, which can be mainly divided into four categories and summarized in Tab. 2.

- **Traditional Graphics.** As representative early implementations, traditional graphics methods in the implementation path can be divided into two categories: **1)** Key information matching and fusion. Methods [174], [178], [196] grounded in critical information matching and fusion are geared towards substituting corresponding regions by aligning key points within facial regions of interest (ROIs), such as the mouth, eyes, nose, and mouth, between the source and target images. Following this, additional procedures such as boundary blending and lighting adjustments are executed to produce the resulting image. Bitouk *et al.* [174] accomplish automated face replacement by constructing a substantial face database to locate faces with akin poses and lighting conditions for substitution. Meanwhile, Nirkin *et al.* [178] enhance keypoint matching and segmentation accuracy by incorporating a Fully Convolutional Network (FCN) into their method. **2)** The construction of a 3D prior model for facial parameterization. Methods [173], [175] based on constructing a 3D prior and introducing a facial parameter model often involve building a facial parameter model using 3DMM technology

TABLE 2: Overview of representative face swapping methods. Notations: ❶ Self-build, ❷ CelebA-HQ, ❸ FFHQ, ❹ VGGFace2, ❺ VGGFace, ❻ CelebV, ❼ CelebA, ❼ VoxCeleb2, ❼ LFW, ❼ KoDF. Abbreviations: SIGGRAPH (SIG.), EUROGRAPHICS (EG.), GANs (G.), VAEs (V.), Diffusion (D.), Split-up and Integration (SI.). Full table can be viewed in Appendix B.

	Method	Venue	Dataset	Categorize	Limitation	Highlight
Traditional Graphics	Blanz <i>et al.</i> [173]	EG'04	❶	3DMM	Manual intervention, unnatural output.	Early face-swapping efforts simplified manual interaction steps.
	Bitouk <i>et al.</i> [174]	SIG'08	❶	SI.	Manual intervention, attribute loss.	A three-phase implementation framework with the help of a pre-constructed face database to match faces that are similar to the source face in terms of posture and lighting.
	Dale <i>et al.</i> [175]	SIG'11	❶	3DMM	Poor generalizability and output quality.	Early work on face exchange, proposing an improved Poisson mixing approach to achieve face swapping in video through frame-by-frame face replacement.
	Lin <i>et al.</i> [176]	ICME'12	[177]	3DMM	Poor generalizability, frequent artifacts.	An attempt to construct a personalized 3D head model to solve the artifact problem occurring in face swapping in large poses.
Generative Adversarial Network	Nirkin <i>et al.</i> [178]	FG'18	[179]	SI.	Poor generalization ability and resolution.	Transfer of expressions and poses by building some 3D variable models and training facial segmentation networks to maintain target facial occlusion.
	RSGAN [117]	SIG'18	❶	G.+V.	Loss of lighting information.	Using two independent VAE modules to represent the latent spaces of the face and hair regions, respectively, with the replacement of identity information in the latent space implemented.
	FSGAN [180]	ICCV'19	[181]	G.	Poor ability to preserve face feature attributes.	Two novel loss functions are introduced to refine the stitching in the face fusion phase following the swapping process.
	FaceShifter [182]	CVPR'20	❶❷❸❹	G.	Poor ability to preserve face feature attributes.	Face swapping is realized in two stages, the firstly AEI-Net improves the output image quality level, and the second AEI-Net is targeted to focus on abnormal regions for image recovery.
	Zhu <i>et al.</i> [183]	AAAI'20	❶	G.+V.	Inability to process facial contour information.	First show of the applicability of deepfake to keypoint invariant de-identification work.
	SimSwap [184]	MM'20	❶❷	G.+V.	Poor ability to preserve face feature attributes.	ID modules and weak feature matching loss functions are proposed to find a balance between identity information replacement and attribute information retention.
	MegaFS [185]	CVPR'21	❶❷❸	G.	Poor ability to preserve face feature attributes.	The first method allows for face swapping on images with a resolution of one million pixels.
	FaceInpainter [186]	CVPR'21	❶❷❸❹	G.+3DMM	Poor representation of image details.	A two-stage framework innovatively implements heterogeneous domains face swapping.
	FSGANv2 [187]	TPAMI'22	❶[181]	G.	Unable to process posture differences effectively.	An extension of the FSGAN method that combines Poisson optimization with perceptual loss enhances the output image facial details.
	FSLSD [121]	CVPR'22	❶❷	G.	Poor ability to preserve face feature attributes.	Potential semantic de-entanglement is realized to obtain facial structural attributes and appearance attributes in a hierarchical manner.
Diffusion	Kim <i>et al.</i> [188]	CVPR'22	❶❷	G.	Unable to process posture differences effectively.	An identity embedder is proposed to enhance the training speed under supervision.
	FALCO [10]	CVPR'23	❶❷	G.	Poor ability to handle facial occlusion.	Oriented with privacy-preserving applications, the method directly employs the latent space of pre-trained GANs to achieve the identity of anonymized images while preserving facial attributes.
	BlendFace [13]	ICCV'23	❶❷❸❹	G.	Unable to handle occlusion and extreme lighting.	The identity features obtained from the de-entanglement are fed to the generator as an identity loss function, which guides the generator to generate an image to fit the source image identity information. It consists of face reshaping network and face exchange network, which better solves the influence of the difference between source and target face contours on the face exchange work.
	FlowFace [189]	AAAI'23	❶❷❸❹	G.+3DMM	Altered target image lighting details.	Utilizing a multi-stage identity injection mechanism effectively combines facial features from both the source and target to produce high-fidelity face swapping.
	StableSwap [190]	TMM'24	❶❷	G.+3D	Unable to handle extreme skin color differences.	Claims to be the first diffusion model-based face exchange framework.
	DiffFace [191]	arXiv'22	❶❷	D.	Facial lighting attributes are altered.	Reenvisioning face swapping as conditional inpainting to harness the power of the diffusion model.
	DiffSwap [192]	CVPR'23	❶❷	D.	Poor ability to handle facial occlusion.	A novel facial all-roundr model capable of performing various facial tasks.
	FaceX [114]	arXiv'23	❶❷❸	D.	Unable to handle extreme skin color differences.	Conditional diffusion model introduces identity and expression encoders components, achieving a balance between identity replacement and attribute preservation during the generation process.
	Liu <i>et al.</i> [9]	arXiv'24	❶❷❸	D.	Poor ability to preserve face feature attributes.	Introducing a multiscale generator network focusing on high-quality semantically aware correspondences between source and target faces.
	Cui <i>et al.</i> [193]	CVPR'23	❶❷	Other	Altered target image lighting details.	The identity generator is designed to reconstruct high-resolution images of specific identities, and an attention mechanism is utilized to enhance the retention of identity information.
Alternative	TransFS [194]	FG'23	❶❷❸	Other	Unable to process posture differences effectively.	A Global Residual Attribute-Preserving Encoder (GRAPE) is proposed, and a network flow considering the facial landmarks of the target face was introduced, achieving high-quality face swapping.
	Wang <i>et al.</i> [195]	TMM'24	❶❷	Other	Poor ability to handle facial occlusion.	

based on a pre-collected face database. After matching the facial information of the source image with the constructed face model, specific modifications are made to the relevant parameters of the facial parameter model to generate a completely new face. Dale *et al.* [175] utilize 3DMM to track facial expressions in two videos, enabling face swapping in videos. Some methods [176], [197] have explored scenarios involving significant pose differences between the source and target images. Lin *et al.* [176] constructs a 3D face model from frontal faces, renderable in any pose. Guo *et al.* [197] utilize plane parameterization and affine transformation to establish a one-to-one dense mapping between 2D graphics. Traditional computer graphics methods solve basic face-swapping problems, exploring full automation to enhance generalization. However, these methods are constrained by the need for similarities in pose and lighting between source and target images. They also face challenges like low image resolution, modification of target attributes, and poor performance in extreme lighting and occlusion scenarios.

• **Generative Adversarial Network.** GAN-based methods aim to obtain realistic images generated through adversarial training between the generator and the discriminator, becoming the mainstream face swapping approach. According to different improvement objectives, methods can be classified into seven categories:

1) Early GAN-based methods [48], [183], [198], [199] address issues related to the similarity of pose and lighting between source and target images. DepthNets [198] combines GANs with 3DMM to map the source face to any target geometry, not limited to the geometric shape of the target template. This allows it to be less affected by differences in pose between the source and target faces. However, they face challenges in

generalizing the trained model to unknown faces.

2) Improved Generalizability. To improve the model's generalization, many efforts [118], [180], [184] are made to explore solutions. Combining GANs with VAEs, the model [117], [200] encodes and processes different facial regions separately. FSGAN [180] integrates face reenactment with face swap, designing a facial blending network to mix two faces seamlessly. SimSwap [184] introduces an identity injection module to avoid integrating identity information into the decoder. However, these methods suffer from low resolution and significant attribute loss and need help to handle facial occlusions effectively.

3) Resolution Upgrading. Some methods [185], [201], [202] provide solutions to enhance the resolution of generated images. MegaFS [185] introduces the first single-lens face swapping method at the million-pixel level. The face encoder no longer compresses facial information but represents it in layers, achieving more detailed preservation. StyleIPSB [202] constrains semantic attribute codes within the subspace of StyleGAN, thereby fixing certain semantic information during face swapping to preserve pore-level details.

4) Geometric Detail Preservation. To capture and reproduce more facial geometric details, some methods [189], [203], [204], [205] introduce 3DMM into GANs, enabling the incorporation of 3D priors. HifiFace [203] introduces a novel 3D shape-aware identity extractor, replacing traditional face recognition networks to generate identity vectors that include precise shape information. FlowFace [189] introduces a two-stage framework based on semantic guidance to achieve shape-aware face swapping. FlowFace+ [205] improves upon FlowFace by utilizing a pre-trained Mask Autoencoder to convert face images into a fine-grained representation

space shared between the target and source faces. It further enhances feature fusion for both source and target by introducing a cross-attention fusion module. However, most of the aforementioned methods often struggle to effectively handle occlusion issues.

5) Facial Masking Artifacts. Some methods [180], [182], [206], [207] have partially alleviated the artifacts caused by facial occlusion. FSGAN [180] designs a restoration network to estimate missing pixels. E4S [206] redefines the face-swapping problem as a mask-exchanging problem for specific information. It utilizes a mask-guided injection module to perform face swapping in the latent space of StyleGAN. However, overall, the methods above have not thoroughly addressed the issue of artifacts in generated images under extreme occlusion conditions.

6) Trade-offs between Identity-replacement and Attribute-retention. In addition to the occlusion issues that need further handling, researchers [13], [208] discover that the balance between identity replacement and attribute preservation in generated images seems akin to a seesaw. Many methods [188], [209], [210] explore the equilibrium between identity replacement and attribute retention. InfoSwap [208] aims to decouple identity and attribute information in face swapping by leveraging the information bottleneck theory. It seeks controlled swapping of identity between source and target faces. StyleSwap [209] introduces a novel swapping guidance strategy, the ID reversal, to enhance the similarity of facial identity in the output. Shiohara *et al.* [13] propose BlendFace, using an identity encoder that extracts identity features from the source image and uses it as identity distance loss, guiding the generator to produce facial exchange results.

7) Model Light-weighting is also an important topic with profound implications for the widespread application of models. FastSwap [211] achieves this by innovating a decoder block called Triple Adaptive Normalization (TAN), effectively integrating identity information from the source image and pose information from the target image. XimSwap [12] modifies the design of convolutional blocks and the identity injection mechanism, successfully deploying on STM32H743.

- **Diffusion-based.** The latest studies [9], [114], [191], [192] in this area produce promising generation results. Diff-Swaps [192] redefines the face swapping problem as a conditional inpainting task. Liu *et al.* [9] introduce a multi-modal face generation framework and achieved this by introducing components such as balanced identity and expression encoders to the conditional diffusion model, striking a balance between identity replacement and attribute preservation during the generation process. As a novel facial generalist model, FaceX [114] can achieve various facial tasks, including face swapping and editing. Leveraging the pre-trained StableDiffusion [7] has significantly improved the quality and model training speed.

- **Alternative Techniques.** There are also some methods that stand independently from the above classifications that are discussed here collectively. Fast Face-swap [212] views the identity swap task as a style transfer task, achieving its goals based on VGG-Net. However, this method has poor generalization. Some methods [193], [194] apply the Transformer architecture to face swapping tasks. Leveraging a facial encoder based on the Swin Transformer [57], TransFS [194]

obtains rich facial features, enabling facial swapping in high-resolution images. ReliableSwap [213] enhances the model's identity preservation capabilities by constructing a reliable supervisor called the "cyclic triplet." However, it has limitations in preserving attribute information.

3.1.2 Face Reenactment

This section reviews current methods from four points: 3DMM-based, landmark matching, face feature decoupling, and self-supervised learning. We summarize them in Tab. 3.

- **3DMM-based.** Some methods [14], [218], [219] utilize 3DMM to construct a facial parameter model as an intermediary for transferring information between the source and target. In particular, Face2Face^ρ [218], based on 3DMM, consists of a u-shaped rendering network driven by head pose and facial motion fields and a hierarchical coarse-to-fine motion network guided by landmarks at different scales. However, some methods [214], [215], [216] exhibit visible artifacts in the background when dealing with significant head movements in the input images. To address issues such as incomplete attribute decoupling in facial reproduction tasks, PECHead [219] models facial expressions and pose movements. It combines self-supervised learning of landmarks with 3D facial landmarks and introduces a new motion-aware multi-scale feature alignment module to eliminate artifacts that may arise from facial motion.

- **Landmark Matching.** This kind of methods [15], [220], [223], [224], [225] aim to establish a mapping relationship between semantic objects in the facial regions of the driving source and the target source through landmarks. Based on this mapping relationship [221], [222], the transfer of facial movement information is achieved. In particular, X2Face [220] achieves one-to-one driving of facial expressions and poses for each frame of the character in the driving video and source video. To address the challenge of reproducing large head poses in facial reenactment, Xu *et al.* [15] propose a dual-generator network incorporating a 3D landmark detector into the model. Free-headgan [225] comprises a 3D keypoint estimator, an eye gaze estimator, and a generator built on the HeadGAN architecture. The 3D keypoint estimator addresses the regression of deformations related to 3D poses and expressions. The eye gaze estimator controls eye movement in videos, providing finer details. MetaPortrait [228] achieves accurate distortion field prediction through dense facial keypoint matching and accelerates model training based on meta-learning principles, delivering excellent results on limited datasets.

- **Feature Decoupling.** The latent feature decoupling and driving methods [16], [229], [230], [231], [232] aims to disentangle facial features in the latent space of the driving video, replacing or mapping the corresponding latent information to achieve high-fidelity facial reproduction under specific conditions. HyperReenact [16] uses attribute decoupling, employing a hyper-network to refine source identity features and modify facial poses. StyleMask [231] separates facial pose and expression from the identity information of the source image by learning masks and blending corresponding channels in the pre-trained style space S of StyleGAN2. HiDe-NeRF [230] employs a deformable neural radiance field to represent a 3D scene, with a lightweight deformation module explicitly decoupling facial pose and expression attributes.

TABLE 3: Overview of representative face reenactment methods. Notations: ① Voxceleb, ② Self-build, ③ Voxceleb2, ④ TalkingHead-1KH, ⑤ CelebV-HQ, ⑥ VFHQ, ⑦ RaFD, ⑧ VGGFace, ⑨ CelebV, ⑩ FFHQ. Abbreviations: Expression (Exp).

Method	Venue	Controllable object	Dataset	Highlight
Based on 3DMM				
Face2Face [214]	CVPR'16	Exp, Pose	②	Using 3D facial reconstruction, transfer facial expressions and pose from a driving character to a target character via affine transformation, then generate the final video through rendering techniques.
Kim <i>et al.</i> [215]	TOG'18	Exp, Pose, Blink	②	Using synthesized rendering images of a parameterized face model as input, creating lifelike video frames for the target actor.
Kim <i>et al.</i> [216]	TOG'19	Lip, Exp, Pose	②	Built on a recurrent generative adversarial network, it employs a hierarchical neural face renderer to synthesize realistic video frames.
Head2Head [14]	FG'21	Exp, Pose, Blink, Gaze	②	The model consists of two stages: facial reconstruction and tracking in the first stage, followed by video rendering in the second stage.
HeadGAN [217]	ECCV'21	Exp, Pose	①	Using 3DMM for facial modeling provides a 3D prior to the GAN, effectively guiding the generator to accurately recover pose and expression from the target frame.
Face2Face ^o [218]	ECCV'22	Exp, Pose	①	Decoupling the actor's facial appearance and motion information with two separate encodings allows the network to learn facial appearance and motion priors.
PECHead [219]	CVPR'23	Lip, Exp, Pose	③④⑤	A novel multi-scale feature alignment module for motion perception is proposed to minimize distortion during motion transmission.
Based on Landmark Matching				
X2Face [220]	CVPR'18	Exp, Pose	③	The training is realized in two stages: the first stage guides the generation frames towards the driving frames and the second stage accomplishes the preservation of the source identity information through the identity loss function.
Zakharov <i>et al.</i> [221]	ICCV'19	Exp, Pose	①②	Proposed a meta-learning framework for adversarial generative models, reducing the required training data size.
FReeNet [222]	CVPR'20	Exp, Pose	⑦ [85]	A new triple perceptual loss is proposed to richly reproduce facial details of the face.
Zakharov <i>et al.</i> [223]	ECCV'20	Exp, Pose	③	Decomposed facial information into two layers for modeling: the first layer synthesizes coarse images related to the pose using a small neural network, and the second layer defines texture images unrelated to the pose, containing high-frequency details.
MarioNETte [224]	AAAI'20	Exp, Pose	①②	Introduced image attention blocks, target feature alignment modules, and landmark transformers, enhancing the model's performance when generalizing to unknown individual identities.
DG [15]	CVPR'22	Exp, Pose	①②⑦	A proposed dual generator model network for large pose face reproduction.
Doukas <i>et al.</i> [225]	TPAMI'23	Exp, Pose, Gaze	① [226] [227]	Eye gaze control in the generated video is implemented to further enhance visual realism.
MetaPortrait [228]	CVPR'23	Exp, Pose	③	By establishing dense facial keypoint matching, accurate deformation field prediction is achieved, and the model training is expedited based on the meta-learning philosophy.
Yang <i>et al.</i> [229]	AAAI'24	Exp, Pose	①③④	The facial tri-plane is represented by canonical tri-plane, identity deformation, and motion components, achieving face reenactment without the need for 3D parameter model priors.
Based on Face Feature Decoupling				
HiDe-NeRF [230]	CVPR'23	Lip, Exp, Pose	①③④	High-fidelity and free-viewing talking head synthesis using deformable neural radiation fields.
HyperReenact [16]	ICCV'23	Exp, Pose	①②	Exploiting the effectiveness of hypernetworks in real image inversion tasks and extending them to real image manipulation.
Stylemask [231]	FG'23	Exp, Pose	③	This work optimizes a Mask Network and combines it with StyleGAN2's style potential space S in order to achieve the separation of facial pose and expression of the target image from the identity features of the source image.
Bounareli <i>et al.</i> [232]	IJCV'24	Exp, Pose	①②	In GANs' latent space, head pose and expression changes are decoupled, achieving near-real outputs through real image embedding.
Based on Self-supervised				
ICface [233]	WACV'20	Exp, Pose	①	The model is decoupled and driven by interpretable control signals that can be obtained from multiple sources such as external driving videos and manual controls.
Oorloff <i>et al.</i> [234]	ICCV'23	Lip, Exp, Pose	③	Identity and attribute decomposition are realized in StyleGAN2's latent space, and a cyclic manifold adjustment technique enhances facial reconstruction results.
Xue <i>et al.</i> [235]	TOMM'23	Exp, Pose	①②	High-fidelity facial generation is achieved by using information-rich Projected Normalized Coordinate Code (PNCC) and eye maps, replacing sparse facial landmark representations.

• **Self-supervised Learning.** Self-supervised learning employs supervisory signals inferred from the intrinsic structure of the data, reducing the reliance on external data labels [233], [234], [236], [237]. Oorloff *et al.* [234] employs self-supervised methods to train an encoder, disentangling identity and facial attribute information of portrait images within the pre-defined latent space itself of a pre-trained StyleGAN2. Zhang *et al.* [237] utilizes 3DMM to provide geometric guidance, employs pre-computed optical flow to guide motion field estimation, and relies on pre-computed occlusion maps to guide the perception and repair of occluded areas.

3.1.3 Talking Face Generation

In this section, we review current methods from three perspectives: audio/text driven, multimodal conditioned, diffusion-based, and 3D-model Technologies. We also summarize them in Tab. 4.

• **Audio/Text Driven.** Methods aim to map and guide lip and facial movements in generated videos by understanding the semantic information from the driving source [243], [255], [259]. Early methods [105], [119] perform poorly in terms of generalization and training complexity. After training, the models struggled to generalize to new individuals, requiring extensive conversational data for training new characters. Researchers [106], [120] propose their solutions from various perspectives. However, Most of these methods prioritize generating lip movements aligned with semantic information, overlooking essential aspects like identity and style, such as head pose changes and movement control, which are crucial in natural videos. To address this, MakeItTalk [238] decouples input audio information by predicting facial landmarks based on audio and obtaining semantic details on facial expressions and poses from audio signals. SadTalker [241] extracts 3D motion coefficients for constructing a 3DMM from audio and uses this to modulate a new 3D perceptual facial rendering for generating head poses in talking videos. Additionally,

some methods [97], [260], [261], [262] propose their improvement methods, and these will not be detailed one by one. In addition, the emotional expression varies for different texts during a conversation, and vivid emotions are an essential part of real talking face videos [240], [263]. Recently, some methods [264], [265], [266] extend their previous approaches by incorporating matching between the driving information and corresponding emotions. EMMN [264] establishes an organic relationship between emotions and lip movements by extracting emotion embeddings from the audio signal, synthesizing overall facial expressions in talking faces rather than focusing solely on audio for facial expression synthesis. AMIGO [265] employs a sequence-to-sequence cross-modal emotion landmark generation network to generate vivid landmarks aided by audio information, ensuring that lips and emotions in the output image sequence are synchronized with the input audio. However, existing methods still lack effective control over the intensity of emotions. In addition, TalkCLIP [267] introduces style parameters, expanding the style categories for text-guided talking video generation. Zhong *et al.* [268] propose a two-stage framework, incorporating appearance priors during the generation process to enhance the model's ability to preserve attributes of the target face. DR2 [19] explores practical strategies for reducing the training workload.

• **Multimodal Conditioned.** To generate more realistic talking videos, some methods [244], [245], [247], [248] introduce additional modal information on top of audio-driven methods to guide facial pose and expression. GC-AVT [245] generates realistic talking videos by independently controlling head pose, audio information, and facial expressions. This approach introduces an expression source video, providing emotional information during the speech and the pose source video. However, the video quality falls below expectations, and it struggles to handle complex background changes.

TABLE 4: Overview of representative talking face generation methods. Notations: ❶ LRW, ❷ VoxCeleb2, ❸ MEAD, ❹ Self-build, ❺ LRS2, ❻ HDTF, ❻ LRS3, ❻ CREMA-D, ❻ VoxCeleb, ❻ FFHQ. Full table can be viewed in Appendix B.

	Method	Venue	Dataset	Limitation	Highlight
Audio / Text - Driven	Chen <i>et al.</i> [120]	CVPR'19	❶	Inability to control pose and emotional variations.	Proposed a cascaded approach, using facial landmarks as an intermediate high-level representation.
	Wav2Lip [106]	ICMR'20	❶❷❸	Poor resolution, inability to control pose and emotional.	A new evaluation framework and a dataset for training mouth synchronization are proposed.
	MakelTalk [238]	TOG'20	❷	Uable to control pose and emotional variations well.	Separating content information and identity information from audio signals, combining LSTM and self-attention mechanism to enhance head movement coherence.
	Ji <i>et al.</i> [239]	CVPR'21	❶❸	Inability to control pose and emotional variations.	By breaking down the input audio sample into content and emotion embeddings, cross-reconstruction of emotional disentanglement creates facial landmarks with nuanced emotional content.
	Gan <i>et al.</i> [240]	ICCV'23	❶❷❸	Insufficient emotional output diversity.	Proposed a two-stage architecture, implementing speaker generation independent of emotion and embedding emotion information.
	SadTalker [241]	CVPR'23	❶❷	Lack emotional and other latent attributes control.	Based on the idea of 3DMM and conditional VAE, 3D coefficients controlling facial motion and expression are generated from audio to realize the reproduction of accurate faces from audio.
	EmoTalk [242]	ICCV'23	❶❷	Poor real-time performance and expression details.	An emotion-entangled encoder and emotion-guided decoder enable emotion injection, with outputs generated using Blendshape and FLAME model rendering.
	TalkLip [243]	CVPR'23	❶❷	Inability to control pose and emotional variations.	Pre-trained lip-reading experts are employed to penalize incorrect lip-reading predictions in the synthesized videos.
	DR2 [19]	WACV'24	❷	Lack emotional and other latent attributes control.	The model explored effective strategies for reducing the training workload.
	PC-AVS [244]	CVPR'21	❶❷	Lack emotional and other latent attributes control.	Introduction of pose-source video drive compensation to generate head motion in video.
Multimodal	GC-AVT [245]	CVPR'22	❶❷	Poor resolution, unable to handl complex backgrounds.	In addition to the source image, a gesture source, an expression source, and audio are introduced to drive the talking head generation.
	Yu <i>et al.</i> [246]	TMM'22	❷	Lack emotional and other latent attributes control.	Fusion of audio and text inputs for more accurate lip movement and chin posture prediction.
	Xu <i>et al.</i> [247]	CVPR'23	❸	Insufficient control over the intensity of emotional output.	Embedding textual, visual, and auditory emotional modalities into a unified space.
	LipFormer [248]	CVPR'23	❶❷	Poor ability to preserve face feature attributes.	Propose retaining high-quality facial details obtained from pre-training in a codebook format and reproducing them by driving the encoded mapping relationship between audio and lip movements.
	Wang <i>et al.</i> [249]	TPAMI'24	❷❸❹	Unable to delicately control emotions.	Using 3DMM as an intermediate variable to convey facial expressions and head movements, and introducing additional reference videos to extract the desired speaking style.
Diffusion	DAE-Talker [250]	MM'23	❷	High model complexity.	It replaces traditional manually crafted intermediate representations with data-driven latent representations obtained from a DAE.
	Yu <i>et al.</i> [251]	ICCV'23	❶❷	Poor resolution, high model complexity.	Building a corresponding mapping between audio and non-lip representations and training using the diffusion model.
	Stypulkowski [252]	WACV'24	❶❸	High model complexity, short video generation duration.	The model incorporates motion frame and audio embedding information to capture past movements and future expressions, with an emphasis on the mouth region through an additional lip sync loss.
3D-Model	EmoTalker [253]	ICASSP'24	❶❷	High model complexity.	It achieves emotion-editable talking face generation based on a conditional diffusion model.
	AD-NeRF [254]	ICCV'21	❷	Inadequate control of emotions and latent attributes.	The NeRF based approach achieves accurate reproduction of detailed facial components and generates the upper body region.
	DFRF [255]	ECCV'22	❷	Lack of emotional and other latent attributes control.	Combining audio with 3D perceptual features and proposing an facial deformation module.
	AE-NeRF [256]	AAAI'24	❷	Lack emotional and other latent attributes control.	Facial modeling is divided into NeRF related to audio and unrelated to audio to enhance audio-visual lip synchronization and facial detail.
	SyncTalk [257]	CVPR'24	❷	Lack controllable emotional intensity regulation.	The facial sync controller boosts component coordination, and a portrait generator corrects artifacts, enhancing video details.
Ye <i>et al.</i> [258]	ICLR'24	❷ [26]	Lack emotional control and occasional artifacts.	Facial and audio information is separately represented using tri-plane, followed by rendering. The generated results are further optimized based on the super-resolution network.	

Xu *et al.* [247] integrate text, image, and audio-emotional modalities into a unified space to complement emotional content in textual information. Multimodal approaches have significantly enhanced the vividness of generated videos, but there is still room for exploration of organically combining information driven by different sources and modalities.

• **Diffusion-based.** Recently, some methods [17], [18], [250], [253], [269] apply the Diffusion model to the task of talking face generation. For fine-grained talking video generation, DAE-Talker [250] replaces manually crafted intermediate representations, such as facial landmarks and 3DMM coefficients, with data-driven latent representations obtained from a Diffusion Autoencoder (DAE). The image decoder generates video frames based on predicted latent variables. EmoTalker [253] utilizes a conditional diffusion model for emotion-editable talking face generation. It introduces emotion intensity blocks and the FED dataset to enhance the model’s understanding of complex emotions. Very recently, diffusion models are gaining prominence in talking face generation tasks [252] and video generation tasks [148], [270].

• **3D-model Technologies.** 3D models, exemplified by NeRF, are gaining traction in talking face generation [254], [255], [256]. AD-NeRF [254] directly feeds features from the input audio signal into a conditional implicit function to generate a dynamic NeRF. AE-NeRF [256] employs a dual NeRF framework to separately model audio-related regions and audio-independent regions. Furthermore, some methods [257], [258] adopt Tri-Plane [271] to represent facial and audio attributes. SyncTalk [257] models and renders head motion using a tri-plane hash representation, and then further enhances the output quality using a portrait synchronization generator. In the foreseeable future, 3D Gaussian Splatting [272] will also be widely applied to this task.

3.1.4 Facial Attribute Editing

In this section, we review current methods chronologically, following the progression in overcoming technical challenges, primarily focusing on multiple attribute editing methods utilizing GANs. Finally, we summarize methods in Tab. 5.

• **Comprehensive Editing.** Facial attribute editing aims to selectively alter specific facial attributes without affecting others. Therefore, disentangling different facial attributes is a primary challenge. Early facial attribute editing models [273], [289] often achieve editing for a single attribute through data-driven training. For instance, Shen *et al.* [289] propose learning the difference between pre-/post-operation images, represented as residual images, to achieve attribute-specific operations. However, single-attribute editing falls short of meeting expectations, and compression steps in the process often lead to a significant loss of image resolution, a common issue in early methods. The fundamental challenge in comprehensive editing and unrelated attribute modification is achieving complete attribute disentanglement. Many approaches [275], [276], [277], [290] have explored this. E.g., HifaFace [277] identifies cycle consistency issues as the cause of facial attribute information loss that proposes a wavelet-based method for high-fidelity face editing, while TransEditor [290] introduces a dual-space GAN structure based on the transformer framework that improves image quality and attribute editing flexibility.

• **Irrelevant-attribute Retained.** Another critical aspect of face editing is retaining as much target image information as possible in the generated images [21], [276], [291]. Guided-Style [291] leverages attention mechanisms in StyleGAN [5] for the adaptive selection of style modifications for different image layers. IA-FaceS [21] embeds the face image to be edited into two branches of the model, where one branch calculates high-dimensional component-invariant content embedding to capture facial details, and the other branch pro-

TABLE 5: Overview of representative facial attribute editing methods. Notations: ① FFHQ, ② CelebA, ③ CelebA-HQ, ④ CelebAMask-HQ, ⑤ VoxCeleb, ⑥ CelebAText-HQ, ⑦ LFW, ⑧ MM CelebA-HQ, ⑨ CARLA, ⑩ Multi-PIE. In addition, some abbreviations are used in the table: SIGGRAPH (SIG.), GANs (G.), Diffusion (D.), Transformer (T.). Full table can be viewed in Appendix B.

Method	Venue	Categorize Dataset	Highlight
GeneGAN [273]	BMVC'17	G.	②⑩ In early attribute editing, separate models were trained for specific attributes. The key idea was to reassemble attribute vectors in the latent space, achieving successful editing.
SC-FEGAN [274]	ICCV'19	G.	③ Users can generate high-quality edited output images by freely sketching parts of the source image.
Shen <i>et al.</i> [275]	CVPR'20	G.	② Thoroughly investigated how to encode different semantics in the latent space and explored the disentanglement between various semantics to achieve precise control over facial attributes.
Yao <i>et al.</i> [276]	ICCV'21	G.+T.	③ By integrating explicit decoupling terms and identity-consistent terms into the loss function, the preservation of facial identity information is improved, resulting in high-quality face editing in videos.
HifaFace [277]	CVPR'21	G.	① Proposed a solution based on wavelet transform to address the issue of partial loss of attribute information when generating edited results due to "cyclic consistency" problems.
Preechakul <i>et al.</i> [278]	CVPR'22	D.	① When encoding images, it is divided into semantically meaningful parts and parts that represent the details of the image.
FENeRF [279]	CVPR'22	G.+NeRF	④ The introduction of semantic masks into the conditional radiance field enables finer image textures.
FDNeRF [29]	SIG'22	G.+NeRF	⑤ The introduction of the Conditional Feature Warping (CFW) module addresses the issue of temporal inconsistency caused by dynamic information in the process of face editing in videos.
AnyFace [20]	CVPR'22	G.	⑥⑦ Proposed a dual-branch framework for text-driven facial editing, with coordination achieved between the two branches through a Cross-Modal Distillation (CMD) module.
Huang <i>et al.</i> [280]	CVPR'23	D.	④ Proposed the concept of assisted diffusion, integrating individual multimodalities to explore the complementarity between different modalities.
Ozkan <i>et al.</i> [281]	ICCV'23	G.	① The entangled attribute space is decomposed into conceptual and hierarchical latent spaces, and transformer network encoders are employed to modify information in the latent space.
CIPS-3D++ [282]	TPAMI'23	G.+NeRF	⑨ Replaced the convolutional architecture with an MLP (Multi-Layer Perceptron) architecture to achieve faster rendering speeds.
TG-3DFace [283]	ICCV'23	G.	⑩ For different scenarios, two sets of text-to-face cross-modal alignment methods were designed with specific focuses.
VecGAN++ [284]	TPAMI'23	G.	③ Orthogonal constraint and disentanglement loss are used to decouple attribute vectors in the latent space.
DiffusionRig [285]	CVPR'23	D.	① 3DMM and diffusion model integration propose a two-stage method for learning personalized facial details.
Kim <i>et al.</i> [286]	CVPR'23	D.	⑤ Proposed a method for facial editing in videos based on the diffusion model.
SDGAN <i>et al.</i> [287]	AAAI'24	G.	③ SDGAN introduces a semantic separation generator and a semantic mask alignment strategy, achieving satisfactory preservation of irrelevant details and precise attribute manipulation.
FaceDNeRF [288]	NIPS'24	D.+NeRF	① Creating and editing facial NeRFs with single-view images, text prompts, and target lighting.

vides low-dimensional component-specific embedding for component operations. Additionally, some approaches [28], [29], [279], [282] combine GANs with NeRF [26] for enhanced spatial awareness capabilities. Specifically, FENeRF [279] uses two decoupled latent codes to generate corresponding facial semantics and textures in a 3D volume with spatial alignment sharing the same geometry. CIPS-3D++ [282] enhances the model’s training efficiency with a NeRF-based shallow 3D shape encoder and an MLP-based deep 2D image decoder.

- **Text Driven** facial attribute editing is a crucial application scenario and a recent hot topic in academic research [20], [283], [292], [293]. TextFace [292] introduces text-to-style mapping, directly encoding text descriptions into the latent space of pre-trained StyleGAN. TG-3DFace [283] introduces two text-to-face cross-modal alignment techniques, including global contrastive learning and fine-grained alignment modules, to enhance the high semantic consistency between the generated 3D face and the input text.

- **Diffusion-based** models have been introduced into facial attribute editing [278], [280], [285], [286] and achieve excellent results. Huang *et al.* [280] propose a collaborative diffusion framework, utilizing multiple pre-trained unimodal diffusion models together for multimodal face generation and editing. DiffusionRig [285] conditions the initial 3D face model, which helps preserve facial identity information during personalized editing of facial appearance based on the general facial details prior to the dataset.

3.2 Forgery Detection

In this section, we review current forgery detection techniques based on the type of detection cues, categorizing them into three: Space Domain (Sec. 3.2.1), Time Domain (Sec. 3.2.2), Frequency Domain (Sec. 3.2.3), and Data-Driven (Sec. 3.2.4). We also summarize the detailed information about popular methods in Tab. 6.

3.2.1 Space Domain

- **Image-level Inconsistency.** The generation process of forged images often involves partial alterations rather than

global generation, leading to common local differences in non-globally generated forgery methods. Therefore, some methods focus on differences in image spatial details as criteria for determining whether an image is forged, such as color [31], saturation [312], artifacts [296], [297], [313], gradient variations [30], *etc.* Specifically, RECCE [297] considers shadow generation from a training perspective, utilizing the learned representations on actual samples to identify image reconstruction differences. LGrad [30] utilizes a pre-trained transformation model, converting images to gradients to visualize general artifacts and subsequently classifying based on these representations. In addition, some works focus on detection based on differences in facial and non-facial regions [295], as well as the fine-grained details of image textures [314], [315]. Recently, Ba *et al.* [299] focus not only on the discordance in a single image region but also on the detection of fused local representation information from multiple non-overlapping areas.

- **Local Noise Inconsistency.** Image forgery may involve adding, modifying, or removing content in the image, potentially altering the noise distribution in the image. Detection methods based on noise aim to identify such local or even global differences in the image. Zhou *et al.* [32] propose a dual-stream structure, combining GoogleNet with a triplet network to focus on tampering artifacts and local noise in images. Nguyen *et al.* [316] utilize capsule networks to detect forged pictures and videos in various forgery scenarios. NoiseDF [298] specializes in identifying underlying noise traces left behind in Deepfake videos, introducing an efficient and novel Multi-Head Relative Interaction with depth-wise separable convolutions to enhance detection performance.

3.2.2 Time Domain

- **Abnormal Physiological Information.** Forgery videos often overlook the authentic physiological features of humans, failing to achieve overall consistency with authentic individuals. Therefore, some methods focus on assessing the plausibility of the physiological features of the generated faces in videos. Li *et al.* [91] detect blinking and blink

TABLE 6: Overview of representative forgery detection methods. Notations: ① FF++, ② DFDC, ③ Celeb-DF, ④ Deeperforensics, ⑤ Self-build, ⑥ UADFV, ⑦ Celeb-HQ, ⑧ DFDCp, ⑨ FFHQ, ⑩ DFD. Full table can be viewed in Appendix B.

	Method	Venue	Train	Test	Highlight
Space Domain	Face X-ray [294]	CVPR'20	①	①②③⑩	Focusing on boundary artifacts of face fusion for forgery detection.
	Nirkin <i>et al.</i> [295]	TPAMI'21	①	①②③	Detecting swapped faces by comparing the facial region with its context (non-facial area).
	SBIs [296]	CVPR'22	①	②③⑧⑩	The belief that the more difficult to detect forged faces typically contain more generalized traces of forgery can encourage the model to learn a feature representation with greater generalization ability.
	RECCE [297]	CVPR'22	①	①②③ [92]	Reconstruction learning on real samples to learn common compressed representations of real images.
	LGrad [30]	CVPR'23	⑥	⑤	The gradient is utilized to present generalized artifacts that are fed into the classifier to determine the truth of the image.
	NoiseDF [298]	AAAI'23	①	①②③④	Extracting noise traces and features from cropped faces and background squares in video frames.
Time Domain	Ba <i>et al.</i> [299]	AAAI'24	①②③	①②③	Multiple non-overlapping local representations are extracted from the image for forgery detection. A local information loss function, based on information bottleneck theory, is proposed for constraint.
	FTCN [300]	ICCV'21	①	①②③④ [182]	It is believed that most face video forgeries are generated frame by frame. As each altered face is independently generated, this inevitably leads to noticeable flickering and discontinuity.
	LipForensics [301]	CVPR'21	①	①②③	Concern about temporal inconsistency of mouth movements in videos.
	M2TR [108]	ICMR'22	①	①②③⑩	Capturing local inconsistencies at different scales for forgery detection using a multiscale transformer.
	Gu <i>et al.</i> [302]	AAAI'22	①	①②③ [92]	By densely sampling adjacent frames to pay attention to the inter-frame image inconsistency.
	Yang <i>et al.</i> [34]	TIFS'23	①②③	①②③	Treating detection as a graph classification problem and focusing on the relationship between the local image features across different frames.
Frequency Domain	AVoID-DF [39]	TIFS'23	②⑥ [84]	②⑥ [84]	Multimodal forgery detection using audiovisual inconsistency.
	Choi <i>et al.</i> [303]	CVPR'24	①③④	①③	Focus on the inconsistency of the style latent vectors between frames.
	Xu <i>et al.</i> [304]	IJCV'24	①②③④	①②③④	Forgery detection is conducted by converting video clips into thumbnails containing both spatial and temporal information.
	F ³ -Net [36]	ECCV'20	①	①	A two-branch frequency perception framework with a cross-attention module is proposed.
	FDFL [37]	CVPR'21	①	①	Propose an adaptive frequency feature generation module to extract differential features from different frequency bands in a learnable manner.
	HFI-Net [305]	TIFS'22	①	②③④⑥ [77]	Notice that the forgery flaws used to distinguish between real and fake faces are concentrated in the mid- and high-frequency spectrum.
Data Driven	Guo <i>et al.</i> [306]	TIFS'23	①②	①②③	Designing a backbone network for Deepfake detection with space-frequency interaction convolution.
	Tan <i>et al.</i> [307]	AAAI'24	⑥	①⑤	A lightweight frequency-domain learning network is proposed to constrain classifier operation within the frequency domain.
	Dang <i>et al.</i> [308]	CVPR'20	⑥	③⑥	Utilizing attention mechanisms to handle the feature maps of the detection model.
	Zhao <i>et al.</i> [309]	ICCV'21	①	①②③④⑥⑩	Proposes pairwise self-consistent learning for training CNN to extract these source features and detect deep vacation images.
	Finfer [310]	AAAI'22	①	①③⑥ [92]	Based on an autoregressive model, using the facial representation of the current frame to predict the facial representation of future frames.
	Huang <i>et al.</i> [109]	CVPR'23	①	①②③⑩ [182]	A new implicit identity-driven face exchange detection framework is proposed.
	HiFi-Net [311]	CVPR'23	⑥	⑥	Converting forgery detection and localization into a hierarchical fine-grained classification problem.

frequency in videos as criteria for determining the video's authenticity. Yang *et al.* [94] focuses on the inconsistency of head poses in videos, comparing the differences between head poses estimated using all facial landmarks and those estimated using only the landmarks in the central region.

• **Inter-Frame Inconsistency.** Methods [33], [34], [300], [302], [303], [304] based on inter-frame inconsistency for forgery detection aim to uncover differences in images between adjacent frames or frames with specific temporal spans. Gu *et al.* [302] focus on inter-frame image inconsistency by densely sampling adjacent frames, while Yin *et al.* [33] design a Dynamic Fine-grained Difference Capturing module and a Multi-Scale Spatio-Temporal Aggregation module to cooperatively model spatio-temporal inconsistencies. Yang *et al.* [34] approach DeepFake detection as a graph classification problem, emphasizing the relationship information between facial regions to capture the relationships among local features across different frames. Choi *et al.* [303] discover that the style variables in each frame of Deepfake work change. Based on this, they developed a style attention module to focus on the inconsistency of the style latent variables between frames.

• **Multimodal Inconsistency.** The core idea behind multimodal detection algorithms is to make judgments based on the flow of prior information from multiple attributes rather than solely considering the image or audio differences of individual characteristics in each frame. The consideration of audio-visual modal inconsistency has received extensive research in various methods [38], [39], [317], [318]. POI-Forensics [317] proposes a deep forgery detection method based on audio-visual authentication, utilizing contrastive

learning to learn the most distinctive embeddings for each identity in moving facial and audio segments. AVoID-DF [39] embeds spatiotemporal information in a spatiotemporal encoder and employs a multimodal joint decoder to fuse multimodal features and learn their inherent relationships. Subsequently, a cross-modal classifier is applied to detect disharmonious operations within and between modalities. Agarwal *et al.* [319] describe a forensic technique for detecting fake faces using static and dynamic auditory ear characteristics. Indeed, multimodal detection methods are currently a hotspot in forgery detection research.

3.2.3 Frequency Domain

Frequency domain-based forgery detection methods transform image time-domain information into the frequency domain. Works [36], [37], [305], [307], [320] utilize statistical measures of periodic features, frequency components, and frequency characteristic distributions, either globally or in local regions, as evaluation metrics for forgery detection. Specifically, HFI-Net [305] consists of a dual-branch network and four Global-Local Interaction (GLI) modules. It effectively explores multi-level frequency artifacts, obtaining frequency-related forgery clues for face detection. Tan *et al.* [307] introduce a novel frequency-aware approach called FreqNet, which focuses on the high-frequency information of images and combines it with a frequency-domain learning module to learn source-independent features. Furthermore, some approaches combine spatial, temporal, and frequency domains for joint consideration [306], [321], and Guo *et al.* [306] design a spatial-frequency interaction convolution to construct a novel backbone network for Deepfake detection.

3.2.4 Data Driven

Data-driven forgery detection focuses on learning specific patterns and features from extensive image or video datasets to distinguish between genuine and potentially manipulated images. Some methods [322], [323] believe that images generated by specific models possess unique model fingerprints. Based on this belief, forgery detection can be achieved by focusing on the model’s training. In addition, FakeSpotter [324] introduces the Neuron Coverage Criterion to capture layer-wise neuron activation behavior. It monitors the neural behavior of a deep face recognition system through a binary classifier to detect fake faces. There are also methods [109], [309] that attempt to classify the sources of different components in an image. For instance, Huang *et al.* [109] think that the difference between explicit and implicit identity helps detect face swapping. There are numerous data-driven methods [308], [310], [311], [325], and it is not feasible to discuss each one in detail here.

3.3 Specific Related Domains

In this section, we briefly review related popular tasks beyond the deepfake generation, such as Face Super-resolution (Sec. 3.3.1), Portrait Style Transfer (Sec. 3.3.2), Body Animation (Sec. 3.3.3), and Makeup Transfer (Sec. 3.3.4).

3.3.1 Face Super-resolution

- **Convolutional Neural Networks.** Early works [123], [326], [327] on facial super-resolution based on CNNs aims to leverage the powerful representational capabilities of CNNs to learn the mapping relationship between low-resolution and high-resolution images from training samples. Depending on whether they focus on local details of the image, they can be divided into global methods [122], [123], local methods [326], and mixed methods [327].

- **Generative Adversarial Network.** GAN aims to achieve the optimal output result through an adversarial process between the generator and the discriminator. This type of method [328], [329] currently dominates the field for flexible and efficient architecture.

3.3.2 Portrait Style Transfer

- **Generative Adversarial Network.** The most mature style transfer algorithm is the GAN-based approach [156], [157], [158]. However, due to the relatively poor stability of GANs, it is common for the generated images to contain artifacts and unreasonable components. 3DAvatarGAN [156] bridges the pre-trained 3D-GAN in the source domain with the 2D-GAN trained on an artistic dataset to achieve cross-domain generation. Scenimefy [158] utilizes semantic constraints provided by text models like CLIP to guide StyleGAN generation and applies patch-based contrastive style loss to enhance stylization and fine details further.

- **Diffusion-based** methods [159], [160], [330] represent the generative process of cross-domain image transfer using diffusion processes. DiffusionGAN3D [330] combines 3DGAN [271] with a diffusion model from text to graphics, introducing relative distance loss and learnable tri-planes for specific scenarios to further enhance cross-domain transformation accuracy.

3.3.3 Body Animation

- **Generative Adversarial Network.** GAN-based approaches [146], [147], [331] aim to train a model to generate images whose conditional distribution resembles the target domain, thus transferring information from reference images to target images. CASD [146] is based on a style distribution module using a cross-attention mechanism, facilitating pose transfer between source semantic styles and target poses. VGFlow [331] introduces a visibility-guided flow module to preserve texture and perform style manipulation concurrently. However, existing methods still rely considerably on training samples, and exhibit decreased performance when dealing with actions in rare poses.

- **Diffusion-based.** The task of body animation using diffusion models aims to utilize diffusion processes to generate the propagation and interaction of movements between body parts based on a reference source. This approach [49], [148], [332] represents a current hot topic in research and implementation. LEO [148] focuses on the spatiotemporal continuity between generated actions, employing the Latent Motion Diffusion Model to represent motion as a series of flow graphs during the generation process. Animate Anyone [332] harnesses the powerful generation capabilities of stable diffusion models combined with attention mechanisms to generate high-quality character animation video.

3.3.4 Makeup Transfer

- **Graphics-based Approaches.** Before the introduction of neural networks, traditional computer graphics methods [333], [334] use image gradient editing and physics-based operations to understand the semantics of makeup. By decomposing the input image into multiple layers, each representing different facial information, traditional methods would distort the reference facial image onto the non-makeup target using facial landmarks for each layer. However, due to the limitations of manually designed operators, the output images from traditional methods often appear unnatural, with noticeable artifacts. Additionally, there is a tendency for background information to be modified to some extent.

- **Generative Adversarial Network.** Early deep learning-based methods [164] aim at fully automatic makeup transfer. However, these methods [163], [335] exhibit poor performance when faced with significant differences in pose and expression between the source and target faces and are unable to handle extreme makeup scenarios well. Some methods [161], [165], [166] proposes their solutions, PSGAN++ [165] comprises the Makeup Distillation Network, Attentive Makeup Morphing module, Style Transfer Network, and Identity Extraction Network, further enhancing the ability of PSGAN [161] to perform targeted makeup transfer with detail preservation. ELeGANt [167], CUMTGAN [170], and HT-ASE [162] explore the preservation of detailed information. ELeGANt [167] encodes facial attributes into pyramid feature maps to retain high-frequency information. Matching facial semantic information, which involves rendering makeup styles onto semantically corresponding positions of a target image, is often overlooked. SSAT [336] introduces the SSCFT module and weakly supervised semantic loss for accurate semantic correspondence. SSAT++ [169] further improves color fidelity matching, but

TABLE 7: Results of representative face swapping methods on FF++. Notations: ❶ CelebA-HQ, ❷ FFHQ, ❸ VGGFace, ❹ VGGFace2, ❺ VoxCeleb2.

Methods	Train	Test: FF++			
		ID Ret.(%) \uparrow	Exp Err. \downarrow	Pose Err. \downarrow	FID \downarrow
FaceShifter [182]	❶❷❸	97.38	2.06	2.96	-
SimSwap [184]	❷	92.83	-	1.53	-
FaceInpainter [186]	❶❷❸	97.63	-	2.21	-
HifiFace [203]	❷	98.48	-	2.63	-
RAFSwap [11]	❶	96.70	2.92	2.53	-
Xu <i>et al.</i> [121]	❷	90.05	2.79	2.46	-
DiffSwap [192]	❷	98.54	5.35	2.45	2.16
FlowFace [189]	❶❷❸	99.26	-	2.66	-
FlowFace++ [205]	❶❷❸	99.51	-	2.20	-
StylePSB [202]	❷	95.05	2.23	3.58	-
StyleSwap [209]	❷❸	97.05	5.28	1.56	2.72
WSC-Swap [204]	❶❷❸	99.88	5.01	1.51	-

TABLE 8: Results of representative face reenactment methods on VoxCeleb for the self-reenactment. Notations: ❶ VoxCeleb, ❷ VoxCeleb2, ❸ ETH-Xgaze, ❹ Gaze360 [226], ❺ MPI-IGaze [227], ❻ TalkingHead-1KH. In addition, we use gray to represent data that is partially uncertain.

Methods	Train	Test: VoxCeleb				
		CSIM \uparrow	PSNR \uparrow	LPIPI \downarrow	FID \downarrow	SSIM \uparrow
HyperReenact [16]	❶	0.710	-	0.230	27.10	-
DG [15]	❶	0.831	-	-	22.10	0.761
AVFR-GAN [337]	❶	-	32.20	-	8.48	0.824
Free-HeadGAN [225]	❶❷❸❹	0.810	22.16	0.100	35.40	-
HiDe-NeRF [230]	❶❷❸	0.931	21.90	0.084	-	0.862

both models are complex with high training complexity. In addition, BeautyREC [168], based on the Transformer with long-range visual dependencies, achieves efficient global makeup transfer with significantly reduced overall model parameters compared to previous works.

4 BENCHMARK RESULTS

We evaluate the performance of representative methods for each reviewed field on the most widely used datasets with the data sourced from the original respective papers. Considering the differences in training datasets, testing datasets, and metrics used by different approaches, we strive to compare them fairly in each table to the greatest extent.

4.1 Main Results on Deepfake Generation

We select widely used metrics for each task and tabulate the performance for representative methods.

• **Results on Face Swapping.** Tab. 7 displays the performance evaluation results of some representative models on the Face Swapping task using the FF++ [78] dataset. WSC-Swap [204] captures facial region external attribute information and internal identity information through two independent encoders, which achieves good identity preservation and facial pose retention. However, it exhibits sub-optimal performance in facial expression error metrics.

• **Results on Face Reenactment.** Tab. 8 and Tab. 9 show the performance evaluation results on the VoxCeleb [71] dataset for self-reenactment and cross-subject reenactment, respectively. AVFR-GAN [337] achieves better performance by using the multimodal modeling. Tab. 10 presents quality assessment results on the VoxCeleb2 dataset.

• **Results on Talking Face Generation.** Tab. 11 displays the performance results of various talking face generation approaches on the MEAD [75] dataset since 2023. AMIGO [265] achieves promising results among all methods.

TABLE 9: Results of representative face reenactment methods on VoxCeleb for the cross-identity reenactment. Notations: ❶ VoxCeleb, ❷ VoxCeleb2, ❸ ETH-Xgaze, ❹ Gaze360 [226], ❺ MPIIGaze [227], ❻ TalkingHead-1KH.

Methods	Train	Test : VoxCeleb				
		CSIM \uparrow	AVD \downarrow	AUCON \uparrow	FID \downarrow	AGD \downarrow
HyperReenact [16]	❶	0.680	-	-	-	-
AVFR-GAN [337]	❶	-	-	-	9.05	-
Free-HeadGAN [225]	❶❷❸❹	0.789	-	-	53.90	13.1
HiDe-NeRF [230]	❶❷❸	0.786	0.012	0.971	57.00	-

TABLE 10: Results of representative face reenactment methods on VoxCeleb2 for quality assessment. Notations: ❶ VoxCeleb, ❷ VoxCeleb2, ❸ LRW, ❹ CelebV-HQ, ❺ TalkingHead-1KH.

Methods	Train	Test: VoxCeleb2				
		CSIM \uparrow	PSNR \uparrow	LMD \downarrow	FID \downarrow	SSIM \uparrow
PC-AVS [244]	❷❸	-	-	-	6.880	-
GC-AVT [245]	❷	-	-	-	2.757	-
Wang <i>et al.</i> [97]	❷	-	28.92	1.830	-	0.830
PECHead [219]	❷❸❹	1.590	-	-	23.05	-
DG [15]	❶	0.721	-	-	51.79	0.540
HiDe-NeRF [230]	❶❸	0.787	-	-	61.00	-

TABLE 11: Evaluation results of the models involved in talking face generation on the MEAD dataset. Notations: ❶ MEAD, ❷ LRW, ❸ VoxCeleb2, ❹ HDTF.

Method	Train	Test: MEAD				
		CSIM \uparrow	LMD \downarrow	M/F-LMD \downarrow	Sync \uparrow	FID \downarrow
Xu <i>et al.</i> [247]	❶	0.83	2.36	-	3.500	15.91
EMMN [264]	❷❸	-	2.780/2.870	3.570	-	30.09/0.850
AMIGO [265]	❷❸	-	2.44	2.140/2.440	-	30.29/0.820
SLIGO [263]	❶	0.88	1.83	-	3.690	-
Gan <i>et al.</i> [240]	❷❸	-	2.250/2.470	-	19.69	21.75/0.680
DreamTalk [18]	❷❸❹	-	2.910/1.930	3.780	-	-
SPACE [266]	❷❸	-	-	3.610	11.68	-
TalkCLIP [267]	❶	-	3.601/2.415	3.773	-	-

TABLE 12: FID evaluation of different methods. Notations: ❶ FFHQ, ❷ CelebA-HQ, ❸ MM CelebA-HQ, ❹ CelebA, ❺ CelebAText-HQ, ❻ Self-build.

Methods	Type	Train	Test	FID \downarrow
FENeRF [279]	GANs+NeRF	❶	❷	12.10
FENeRF [279]	GANs+NeRF	❶	❶	28.20
AnyFace [20]	GANs	❷	❸	56.75
AnyFace [20]	GANs	❷	❷	50.56
TextFace [292]	GANs	❷	❷	22.81
TG-3DFace [283]	GANs	❸	❸	52.21
TG-3DFace [283]	GANs	❸	❸	39.02
HifaFace [277]	GANs	❶❷	❶❷	4.04
GuidedStyle [291]	GANs	❷	❶	41.79

• **Results on Facial Attribute Editing.** Tab.12 evaluates the quality level of generated images using FID, and Tab.13 assesses facial reconstruction capabilities using PSNR, LPIPS, and SSIM. Due to different training and testing datasets, quantitative fair comparisons are not possible that just serve as performance demonstrations.

4.2 Main Results on Forgery Detection

The mainstream evaluation metrics for forgery detection technology are ACC and AUC. Tab. 14 presents the ACC and AUC metrics for some detection models trained on FF++ [78] and tested on FF++ (HQ) and FF++ (LQ). LipForensics [301] exhibits robust performance on the strongly compressed FF++ (LQ), while Guo *et al.* [325] perform best on FF++ (HQ). Tab. 15 shows the cross-dataset evaluation using DFDC [82], Celeb-DF [83], Celeb-DFv2 [83], and DeeperForensics-1.0 [81] as validation sets. AVoID-DF [39] and Zhao *et al.* [309] demonstrate excellent generalization ability, but there is still significant room for improvement in these datasets.

TABLE 13: Results of facial reconstruction capabilities in facial attribute editing work. Notations: ① FFHQ, ② VoxCeleb, ③ VoxCeleb2, ④ CelebA-HQ.

Methods	Type	Train	Test	PSNR↑	LPIPS↓	SSIM↑
Preechakul <i>et al.</i> [278]	Difussion	①	④	-	0.0110	0.991
Kim <i>et al.</i> [286]	Difussion	①	①	-	0.0450	0.922
FDNeRF [29]	GANs+NeRF	①	①	-	0.1420	0.821
IA-FaceS [21]	GANs	①④	④	22.34	0.2240	0.642
IA-FaceS [21]	GANs	①④	①	22.43	0.0384	0.659

TABLE 14: Results of the self-dataset performance on FF++. Notations: HQ (Mild compression), LQ (Heavy compression).

Methods	Train	FF++ (LQ)		FF++ (HQ)	
		ACC(%)	AUC(%)	ACC(%)	AUC(%)
F ³ -Net [36]	FF++	93.02	95.80	98.95	99.30
Masi <i>et al.</i> [321]	FF++	86.34	-	96.43	-
Zhao <i>et al.</i> [313]	FF++	88.69	90.40	97.60	99.29
FDFL [37]	FF++	89.00	92.40	96.69	99.30
LipForensics [301]	FF++	94.20	98.10	98.80	99.70
RECCE [297]	FF++	91.03	95.02	97.06	99.32
Guo <i>et al.</i> [325]	FF++	92.76	96.85	99.24	99.75
MRL [34]	FF++	91.81	96.18	93.82	98.27

TABLE 15: Results of cross-dataset performance evaluation on four datasets DFDC, Celeb-DF (CDF), Celeb-DFv2 (CDFv2), and DeeperForensics-1.0 (DFo). Evaluation indicator is AUC. Notations: ① FF++, ② FF++(Real), ③ FF++(HQ), ④ FF++(LQ), ⑤ Self-build, ⑥ SR-DF [108], ⑦ DFDCp, ⑧ FakeAVCeleb, ⑨ DefakeAVMiT.

Methods	Train	DFDC	CDF	CDFv2	DFo
Face X-ray [294]	①⑤	80.92	80.58	-	-
Face X-ray [294]	⑤	71.15	74.76	-	-
Masi <i>et al.</i> [321]	⑦	-	73.41	-	-
Zhao <i>et al.</i> [313]	①	67.44	-	-	-
Zhao <i>et al.</i> [309]	②	67.52	98.30	90.03	99.41
Zheng <i>et al.</i> [300]	①	74.00	-	86.90	98.80
LipForensics [301]	①	73.50	-	82.40	97.60
M2TR [108]	⑥	-	82.10	-	-
M2TR [108]	①	-	68.20	-	-
RECCE [297]	①	69.06	68.71	-	-
SBIs [296]	⑦	-	-	90.79	-
SBIs [296]	①	72.42	-	93.18	-
RealForensics [38]	①	75.90	-	86.90	99.30
Guo <i>et al.</i> [325]	③	81.65	84.97	-	-
Yin <i>et al.</i> [33]	④	73.08	71.36	-	-
MRL [34]	④	71.53	83.58	-	-
AVoID-DF [39]	⑧	80.60	-	-	-
AVoID-DF [39]	⑨	90.30	-	-	-

5 FUTURE PROSPECTS

This section provides a short discussion of future research directions that can facilitate and envision the development of deepfake generation and detection.

• **Face Swapping.** Generalization is a significant issue in face swapping models. While many models demonstrate excellent performance on their training sets, there is often noticeable performance degradation when applied to different datasets during testing. In addition, beyond the common evaluation metrics, various face swapping works employ different evaluation metric systems, lacking a unified evaluation protocol. This absence hinders researchers from intuitively assessing model performance. Therefore, establishing comprehensive experimental and evaluation frameworks is crucial for fair comparisons, and driving progress in the field.

• **Face Reenactment.** Existing methods have room for improvement, facing three main challenges: convenience, authenticity, and security. Many approaches struggle to balance lightweight deployment and generating high-quality

reenactment effects, hindering the widespread adoption of facial reenactment technology in industries. Moreover, several methods claim to achieve high-quality facial reenactment, but they exhibit visible degradation in output during rapid pose changes or extreme lighting conditions in driving videos. Additionally, the computational complexity, consuming significant time and system resources, poses substantial challenges for practical applications.

• **Talking Face Generation.** Current methods strive to enhance the realism of generated conversational videos. However, they lack fine-grained control over the emotional nuances of the conversation, where the matching of emotional intonation to audio and semantic content is not precise enough, and the control over emotional intensity is too coarse. In addition, the realistic correlation between head pose and facial expression movement seems insufficiently considered. Lastly, for text or audio with intense emotions, noticeable artifacts in head movement still occur to a significant extent.

• **Facial Attribute Editing.** Currently, mainstream facial attribute editing employs the decoupling concept based on GANs, and diffusion models are gradually being introduced into this field. The primary challenge is effectively separating the facial attributes to prevent unintended processing of other facial features during attribute editing. Additionally, there needs to be a universally accepted benchmark dataset and evaluation framework for fair assessments of facial editing.

• **Forgery Detection.** With the rapid development of facial forgery techniques, the central challenge in face forgery detection technology is accurately identifying various forgery methods using a single detection model. Simultaneously, ensuring that the model exhibits robustness when detecting forgeries in the presence of disturbances such as compression is crucial. Most detection models follow a generic approach targeting common operational steps of a specific forgery method, such as the integration phase in face swapping or assessing temporal inconsistencies, but this manner limits the model’s generalization capabilities. Moreover, as forgery techniques evolve, forged videos may evade detection by introducing interference during the detection process.

6 CONCLUSION

This survey comprehensively reviews the latest developments in the field of deepfake generation and detection, which is the first to cover a variety of related fields thoroughly and discusses the latest technologies such as diffusion. Specifically, this paper covers an overview of basic background knowledge, including concepts of research tasks, the development of generative models and neural networks, and other information from closely related fields. Subsequently, we summarize the technical approaches adopted by different methods in the mainstream four generation and one detection fields, and classify and discuss the methods from a technical perspective. In addition, we strive to fairly organize and benchmark the representative methods in each field. Finally, we summarize the current challenges and future research directions for each field.

Acknowledgement. This work is supported by the National Natural Science Foundation of China (No. 62371189).

REFERENCES

[1] T. Sha, W. Zhang, T. Shen, Z. Li, and T. Mei, "Deep person generation: A survey from the perspective of face, pose, and cloth synthesis," *CSUR*, 2023. [1](#), [2](#)

[2] D. P. Kingma and M. Welling, "Auto-encoding variational bayes," *stat*, 2014. [1](#), [3](#), [4](#)

[3] K. Sohn, H. Lee, and X. Yan, "Learning structured output representation using deep conditional generative models," in *NeurIPS*, 2015. [1](#), [3](#)

[4] A. Van Den Oord, O. Vinyals *et al.*, "Neural discrete representation learning," in *NeurIPS*, 2017. [1](#), [3](#)

[5] T. Karras, S. Laine, and T. Aila, "A style-based generator architecture for generative adversarial networks," in *CVPR*, 2019. [1](#), [3](#), [4](#), [5](#), [9](#)

[6] T. Karras, S. Laine, M. Aittala, J. Hellsten, J. Lehtinen, and T. Aila, "Analyzing and improving the image quality of stylegan," in *CVPR*, 2020. [1](#), [3](#)

[7] A. Blattmann, T. Dockhorn, S. Kulal, D. Mendelevitch, M. Kilian, D. Lorenz, Y. Levi, Z. English, V. Voleti, A. Letts *et al.*, "Stable video diffusion: Scaling latent video diffusion models to large datasets," *arXiv*, 2023. [1](#), [3](#), [7](#)

[8] Y. Guo, C. Yang, A. Rao, Y. Wang, Y. Qiao, D. Lin, and B. Dai, "Animatediff: Animate your personalized text-to-image diffusion models without specific tuning," in *ICLR*, 2024. [1](#), [3](#)

[9] R. Liu, B. Ma, W. Zhang, Z. Hu, C. Fan, T. Lv, Y. Ding, and X. Cheng, "Towards a simultaneous and granular identity-expression control in personalized face generation," *arXiv*, 2024. [1](#), [6](#), [7](#), [23](#)

[10] S. Barattin, C. Tzelepis, I. Patras, and N. Sebe, "Attribute-preserving face dataset anonymization via latent code optimization," in *CVPR*, 2023. [1](#), [6](#), [23](#)

[11] C. Xu, J. Zhang, M. Hua, Q. He, Z. Yi, and Y. Liu, "Region-aware face swapping," in *CVPR*, 2022. [1](#), [13](#), [23](#)

[12] A. Ancilotto, F. Paissan, and E. Farella, "Ximswap: many-to-many face swapping for tinyml," *TECS*, 2023. [1](#), [7](#)

[13] K. Shiohara, X. Yang, and T. Taketomi, "Blendface: Re-designing identity encoders for face-swapping," in *ICCV*, 2023. [1](#), [6](#), [7](#), [23](#)

[14] M. R. Koujan, M. C. Doukas, A. Roussos, and S. Zafeiriou, "Head2head: Video-based neural head synthesis," in *FG*, 2020. [1](#), [7](#), [8](#)

[15] G.-S. Hsu, C.-H. Tsai, and H.-Y. Wu, "Dual-generator face reenactment," in *CVPR*, 2022. [1](#), [7](#), [8](#), [13](#)

[16] S. Bounareli, C. Tzelepis, V. Argyriou, I. Patras, and G. Tzimiropoulos, "Hyperreenact: one-shot reenactment via jointly learning to refine and retarget faces," in *ICCV*, 2023. [1](#), [7](#), [8](#), [13](#)

[17] A. Mir, E. Alonso, and E. Mondragón, "Dit-head: High-resolution talking head synthesis using diffusion transformers," in *ICAART*, 2024. [1](#), [4](#), [9](#)

[18] Y. Ma, S. Zhang, J. Wang, X. Wang, Y. Zhang, and Z. Deng, "Dreamtalk: When expressive talking head generation meets diffusion probabilistic models," *arXiv*, 2023. [1](#), [9](#), [13](#), [24](#)

[19] C. Zhang, C. Wang, Y. Zhao, S. Cheng, L. Luo, and X. Guo, "Dr2: Disentangled recurrent representation learning for data-efficient speech video synthesis," in *WACV*, 2024. [1](#), [8](#), [9](#), [24](#)

[20] J. Sun, Q. Deng, Q. Li, M. Sun, M. Ren, and Z. Sun, "Anyface: Free-style text-to-face synthesis and manipulation," in *CVPR*, 2022. [1](#), [10](#), [13](#), [24](#)

[21] W. Huang, S. Tu, and L. Xu, "Ia-faces: A bidirectional method for semantic face editing," *Neural Networks*, 2023. [1](#), [9](#), [14](#)

[22] Y. Pang, Y. Zhang, W. Quan, Y. Fan, X. Cun, Y. Shan, and D.-m. Yan, "Dpe: Disentanglement of pose and expression for general video portrait editing," in *CVPR*, 2023. [1](#)

[23] I. Goodfellow, J. Pouget-Abadie, M. Mirza, B. Xu, D. Warde-Farley, S. Ozair, A. Courville, and Y. Bengio, "Generative adversarial nets," in *NeurIPS*, 2014. [1](#), [3](#), [4](#)

[24] J. Ho, A. Jain, and P. Abbeel, "Denoising diffusion probabilistic models," in *NeurIPS*, 2020. [1](#), [3](#), [4](#)

[25] R. Rombach, A. Blattmann, D. Lorenz, P. Esser, and B. Ommer, "High-resolution image synthesis with latent diffusion models," in *CVPR*, 2022. [1](#), [3](#)

[26] B. Mildenhall, P. Srinivasan, M. Tancik, J. Barron, R. Ramamoorthi, and R. Ng, "Nerf: Representing scenes as neural radiance fields for view synthesis," in *ECCV*, 2020. [1](#), [4](#), [10](#)

[27] K. Gao, Y. Gao, H. He, D. Lu, L. Xu, and J. Li, "Nerf: Neural radiance field in 3d vision, a comprehensive review," *arXiv*, 2022. [1](#), [4](#)

[28] K. Jiang, S.-Y. Chen, F.-L. Liu, H. Fu, and L. Gao, "Nerffaceediting: Disentangled face editing in neural radiance fields," in *SIGGRAPH*, 2022. [1](#), [10](#)

[29] J. Zhang, X. Li, Z. Wan, C. Wang, and J. Liao, "Fdnerf: Few-shot dynamic neural radiance fields for face reconstruction and expression editing," in *SIGGRAPH*, 2022. [1](#), [10](#), [14](#), [24](#)

[30] C. Tan, Y. Zhao, S. Wei, G. Gu, and Y. Wei, "Learning on gradients: Generalized artifacts representation for gan-generated images detection," in *CVPR*, 2023. [1](#), [4](#), [10](#), [11](#), [25](#)

[31] P. He, H. Li, and H. Wang, "Detection of fake images via the ensemble of deep representations from multi color spaces," in *ICIP*, 2019. [1](#), [10](#)

[32] P. Zhou, X. Han, V. I. Morariu, and L. S. Davis, "Two-stream neural networks for tampered face detection," in *CVPRW*, 2017. [1](#), [10](#)

[33] Q. Yin, W. Lu, B. Li, and J. Huang, "Dynamic difference learning with spatio-temporal correlation for deepfake video detection," *TIFS*, 2023. [1](#), [11](#), [14](#)

[34] Z. Yang, J. Liang, Y. Xu, X.-Y. Zhang, and R. He, "Masked relation learning for deepfake detection," *TIFS*, 2023. [1](#), [11](#), [14](#), [25](#)

[35] H. Ilyas, A. Javed, and K. M. Malik, "Avfakenet: A unified end-to-end dense swin transformer deep learning model for audio-visual deepfakes detection," *Applied Soft Computing*, 2023. [1](#)

[36] Y. Qian, G. Yin, L. Sheng, Z. Chen, and J. Shao, "Thinking in frequency: Face forgery detection by mining frequency-aware clues," in *ECCV*, 2020. [1](#), [11](#), [14](#), [25](#)

[37] J. Li, H. Xie, J. Li, Z. Wang, and Y. Zhang, "Frequency-aware discriminative feature learning supervised by single-center loss for face forgery detection," in *CVPR*, 2021. [1](#), [11](#), [14](#), [25](#)

[38] A. Haliassos, R. Mira, S. Petridis, and M. Pantic, "Leveraging real talking faces via self-supervision for robust forgery detection," in *CVPR*, 2022. [1](#), [11](#), [14](#)

[39] W. Yang, X. Zhou, Z. Chen, B. Guo, Z. Ba, Z. Xia, X. Cao, and K. Ren, "Avoid-df: Audio-visual joint learning for detecting deepfake," *TIFS*, 2023. [1](#), [11](#), [13](#), [14](#), [25](#)

[40] Y. Mirsky and W. Lee, "The creation and detection of deepfakes: A survey," *CSUR*, 2021. [2](#)

[41] K. Vyas, P. Pareek, R. Jayaswal, and S. Patil, "Analysing the landscape of deep fake detection: A survey," *IJISAE*, 2024. [2](#)

[42] Y. Liu, Q. Li, Q. Deng, Z. Sun, and M.-H. Yang, "Gan-based facial attribute manipulation," *TPAMI*, 2023. [2](#)

[43] A. Melnik, M. Miasayedzenkau, D. Makaravets, D. Pirshtuk, E. Akbulut, D. Holzmann, T. Renusch, G. Reichert, and H. Ritter, "Face generation and editing with stylegan: A survey," *TPAMI*, 2024. [2](#)

[44] G. Zheng and Y. Xu, "Efficient face detection and tracking in video sequences based on deep learning," *Information Sciences*, 2021. [3](#)

[45] J. Sohl-Dickstein, E. Weiss, N. Maheswaranathan, and S. Ganguli, "Deep unsupervised learning using nonequilibrium thermodynamics," in *ICML*, 2015. [3](#)

[46] M. Mirza and S. Osindero, "Conditional generative adversarial nets," *arXiv*, 2014. [3](#)

[47] P. Isola, J.-Y. Zhu, T. Zhou, and A. A. Efros, "Image-to-image translation with conditional adversarial networks," in *ICCV*, 2017. [3](#)

[48] J. Bao, D. Chen, F. Wen, H. Li, and G. Hua, "Cvae-gan: fine-grained image generation through asymmetric training," in *ICCV*, 2017. [3](#), [6](#)

[49] Y. Ma, Y. He, X. Cun, X. Wang, Y. Shan, X. Li, and Q. Chen, "Follow your pose: Pose-guided text-to-video generation using pose-free videos," *arXiv*, 2023. [3](#), [5](#), [12](#)

[50] J. Liu, Q. Wang, H. Fan, Y. Wang, Y. Tang, and L. Qu, "Residual denoising diffusion models," in *CVPR*, 2024. [3](#)

[51] Y. LeCun, L. Bottou, Y. Bengio, and P. Haffner, "Gradient-based learning applied to document recognition," *Proceedings of the IEEE*, 1998. [3](#), [4](#)

[52] A. Krizhevsky, I. Sutskever, and G. E. Hinton, "Imagenet classification with deep convolutional neural networks," in *NeurIPS*, 2012. [3](#), [4](#), [22](#)

[53] K. He, X. Zhang, S. Ren, and J. Sun, "Deep residual learning for image recognition," in *CVPR*, 2016. [3](#), [4](#)

[54] Z. Liu, H. Mao, C.-Y. Wu, C. Feichtenhofer, T. Darrell, and S. Xie, "A convnet for the 2020s," in *CVPR*, 2022. [3](#), [4](#)

[55] J. Zhang, X. Li, J. Li, L. Liu, Z. Xue, B. Zhang, Z. Jiang, T. Huang, Y. Wang, and C. Wang, "Rethinking mobile block for efficient attention-based models," in *ICCV*, 2023. [3](#)

[56] J. Zhang, X. Li, Y. Wang, C. Wang, Y. Yang, Y. Liu, and D. Tao, "Eatformer: Improving vision transformer inspired by evolutionary algorithm," *IJCV*, 2024. 3

[57] Z. Liu, Y. Lin, Y. Cao, H. Hu, Y. Wei, Z. Zhang, S. Lin, and B. Guo, "Swin transformer: Hierarchical vision transformer using shifted windows," in *ICCV*, 2021. 4, 7

[58] A. Vaswani, N. Shazeer, N. Parmar, J. Uszkoreit, L. Jones, A. N. Gomez, L. Kaiser, and I. Polosukhin, "Attention is all you need," in *NeurIPS*, 2017. 4

[59] A. Dosovitskiy, L. Beyer, A. Kolesnikov, D. Weissenborn, X. Zhai, T. Unterthiner, M. Dehghani, M. Minderer, G. Heigold, S. Gelly *et al.*, "An image is worth 16x16 words: Transformers for image recognition at scale," in *ICLR*, 2021. 4

[60] W. Wang, E. Xie, X. Li, D.-P. Fan, K. Song, D. Liang, T. Lu, P. Luo, and L. Shao, "Pyramid vision transformer: A versatile backbone for dense prediction without convolutions," in *ICCV*, 2021. 4

[61] Z. Liu, H. Hu, Y. Lin, Z. Yao, Z. Xie, Y. Wei, J. Ning, Y. Cao, Z. Zhang, L. Dong *et al.*, "Swin transformer v2: Scaling up capacity and resolution," in *CVPR*, 2022. 4

[62] P. Sharma, A. Tewari, Y. Du, S. Zakharov, R. A. Ambrus, A. Gaidon, W. T. Freeman, F. Durand, J. B. Tenenbaum, and V. Sitzmann, "Neural groundplans: Persistent neural scene representations from a single image," in *ICLR*, 2023. 4

[63] M. Z. Irshad, S. Zakharov, K. Liu, V. Guizilini, T. Kollar, A. Gaidon, Z. Kira, and R. Ambrus, "Neo 360: Neural fields for sparse view synthesis of outdoor scenes," in *ICCV*, 2023. 4

[64] Y. Liu, B. Hu, J. Huang, Y.-W. Tai, and C.-K. Tang, "Instance neural radiance field," in *ICCV*, 2023. 4

[65] Z. Min, B. Zhuang, S. Schulter, B. Liu, E. Dunn, and M. Chandraker, "Neurocs: Neural nocs supervision for monocular 3d object localization," in *CVPR*, 2023. 4

[66] S. Hwang, J. Hyung, D. Kim, M.-J. Kim, and J. Choo, "Faceclip-nerf: Text-driven 3d face manipulation using deformable neural radiance fields," in *ICCV*, 2023. 4

[67] Y. Yang, Y. Yang, H. Guo, R. Xiong, Y. Wang, and Y. Liao, "Urban-giraffe: Representing urban scenes as compositional generative neural feature fields," *arXiv*, 2023. 4

[68] G. B. Huang, M. Mattar, T. Berg, and E. Learned-Miller, "Labeled faces in the wild: A database for studying face recognition in unconstrained environments," in *Workshop on faces in 'Real-Life' Images: detection, alignment, and recognition*, 2008. 4, 5

[69] Z. Liu, P. Luo, X. Wang, and X. Tang, "Deep learning face attributes in the wild," in *ICCV*, 2015. 4, 5, 25

[70] O. Parkhi, A. Vedaldi, and A. Zisserman, "Deep face recognition," in *BMVC*, 2015. 4, 5

[71] A. Nagrani, J. S. Chung, and A. Zisserman, "Voxceleb: a large-scale speaker identification dataset," in *Interspeech*, 2017. 4, 5, 13

[72] T. Karras, T. Aila, S. Laine, and J. Lehtinen, "Progressive growing of gans for improved quality, stability, and variation," in *ICLR*, 2018. 4, 5

[73] Q. Cao, L. Shen, W. Xie, O. M. Parkhi, and A. Zisserman, "Vggface2: A dataset for recognising faces across pose and age," in *FG*, 2018. 4, 5

[74] J. S. Chung, A. Nagrani, and A. Zisserman, "Voxceleb2: Deep speaker recognition," in *Interspeech*, 2018. 4, 5

[75] K. Wang, Q. Wu, L. Song, Z. Yang, W. Wu, C. Qian, R. He, Y. Qiao, and C. C. Loy, "Mead: A large-scale audio-visual dataset for emotional talking-face generation," in *ECCV*, 2020. 4, 5, 13

[76] H. Zhu, W. Wu, W. Zhu, L. Jiang, S. Tang, L. Zhang, Z. Liu, and C. C. Loy, "Celebvh-q: A large-scale video facial attributes dataset," in *ECCV*, 2022. 4, 5, 9, 24

[77] P. Korshunov and S. Marcel, "Deepfakes: a new threat to face recognition? assessment and detection," *arXiv*, 2018. 4, 5, 11, 25

[78] A. Rossler, D. Cozzolino, L. Verdoliva, C. Riess, J. Thies, and M. Nießner, "Faceforensics++: Learning to detect manipulated facial images," in *ICCV*, 2019. 4, 5, 13

[79] B. Dolhansky, R. Howes, B. Pflaum, N. Baram, and C. C. Ferrer, "The deepfake detection challenge (dfdc) preview dataset," *arXiv*, 2019. 4, 5

[80] DFD, "Dfd," <https://blog.research.google/2019/09/contributing-data-to-deepfake-detection.html>, 2019. 4, 5

[81] L. Jiang, R. Li, W. Wu, C. Qian, and C. C. Loy, "Deepforensics-1.0: A large-scale dataset for real-world face forgery detection," in *CVPR*, 2020. 4, 5, 13

[82] B. Dolhansky, J. Bitton, B. Pflaum, J. Lu, R. Howes, M. Wang, and C. C. Ferrer, "The deepfake detection challenge (dfdc) dataset," *arXiv*, 2020. 4, 5, 13

[83] Y. Li, X. Yang, P. Sun, H. Qi, and S. Lyu, "Celeb-df: A large-scale challenging dataset for deepfake forensics," in *CVPR*, 2020. 4, 5, 13

[84] H. Khalid, S. Tariq, M. Kim, and S. S. Woo, "Fakeavceleb: A novel audio-video multimodal deepfake dataset," in *NeurIPS*, 2021. 4, 5, 11, 25

[85] S. Moore and R. Bowden, "Multi-view pose and facial expression recognition," in *BMVC*, 2010. 4, 8

[86] W. Xia, Y. Yang, J.-H. Xue, and B. Wu, "Tedigan: Text-guided diverse face image generation and manipulation," in *CVPR*, 2021. 4

[87] J. Sun, Q. Li, W. Wang, J. Zhao, and Z. Sun, "Multi-caption text-to-face synthesis: Dataset and algorithm," in *ACM MM*, 2021. 4

[88] T.-C. Wang, A. Mallya, and M.-Y. Liu, "One-shot free-view neural talking-head synthesis for video conferencing," in *CVPR*, 2021. 4

[89] T. Afouras, J. S. Chung, A. Senior, O. Vinyals, and A. Zisserman, "Deep audio-visual speech recognition," in *TPAMI*, 2018. 4, 24

[90] T. Afouras, J. S. Chung, and A. Zisserman, "Lrs3-ted: a large-scale dataset for visual speech recognition," *arXiv*, 2018. 4

[91] Y. Li, M.-C. Chang, and S. Lyu, "In ictu oculi: Exposing ai generated fake face videos by detecting eye blinking," in *WIFS*, 2018. 4, 10, 25

[92] B. Zi, M. Chang, J. Chen, X. Ma, and Y.-G. Jiang, "Wilddeepfake: A challenging real-world dataset for deepfake detection," in *ACM MM*, 2020. 4, 11, 25

[93] P. Kwon, J. You, G. Nam, S. Park, and G. Chae, "Kodf: A large-scale korean deepfake detection dataset," in *ICCV*, 2021. 4

[94] X. Yang, Y. Li, and S. Lyu, "Exposing deep fakes using inconsistent head poses," in *ICASSP*, 2019. 4, 11, 25

[95] K. Narayan, H. Agarwal, K. Thakral, S. Mittal, M. Vatsa, and R. Singh, "Deephy: On deepfake phylogeny," in *IJCB*, 2022. 4

[96] —, "Df-platter: multi-face heterogeneous deepfake dataset," in *CVPR*, 2023. 4

[97] J. Wang, Y. Zhao, H. Fan, T. Xu, Q. Li, S. Li, and L. Liu, "Memory-augmented contrastive learning for talking head generation," in *ICASSP*, 2023. 4, 8, 13

[98] Z. Wang, A. C. Bovik, H. R. Sheikh, and E. P. Simoncelli, "Image quality assessment: from error visibility to structural similarity," *TIP*, 2004. 4, 22

[99] R. Zhang, P. Isola, A. A. Efros, E. Shechtman, and O. Wang, "The unreasonable effectiveness of deep features as a perceptual metric," in *CVPR*, 2018. 4, 22

[100] M. Heusel, H. Ramsauer, T. Unterthiner, B. Nessler, and S. Hochreiter, "Gans trained by a two time-scale update rule converge to a local nash equilibrium," in *NeurIPS*, 2017. 4, 22

[101] M. Bińkowski, D. J. Sutherland, M. Arbel, and A. Gretton, "Demystifying mmd gans," in *ICLR*, 2018. 4, 22

[102] H. Wang, Y. Wang, Z. Zhou, X. Ji, D. Gong, J. Zhou, Z. Li, and W. Liu, "Cosface: Large margin cosine loss for deep face recognition," in *CVPR*, 2018. 4, 22

[103] B. Chaudhuri, N. Vesdapunt, and B. Wang, "Joint face detection and facial motion retargeting for multiple faces," in *CVPR*, 2019. 4

[104] N. Ruiz, E. Chong, and J. M. Rehg, "Fine-grained head pose estimation without keypoints," in *CVPR*, 2018. 4, 22

[105] L. Chen, Z. Li, R. K. Maddox, Z. Duan, and C. Xu, "Lip movements generation at a glance," in *ECCV*, 2018. 4, 8, 22, 24

[106] K. Prajwal, R. Mukhopadhyay, V. P. Namboodiri, and C. Jawahar, "A lip sync expert is all you need for speech to lip generation in the wild," in *ACM MM*, 2020. 4, 8, 9, 22, 24

[107] B. M. Le and S. S. Woo, "Quality-agnostic deepfake detection with intra-model collaborative learning," in *ICCV*, 2023. 4

[108] J. Wang, Z. Wu, W. Ouyang, X. Han, J. Chen, Y.-G. Jiang, and S.-N. Li, "M2tr: Multi-modal multi-scale transformers for deepfake detection," in *ICML*, 2022. 4, 11, 14, 25

[109] B. Huang, Z. Wang, J. Yang, J. Ai, Q. Zou, Q. Wang, and D. Ye, "Implicit identity driven deepfake face swapping detection," in *CVPR*, 2023. 4, 11, 12, 25

[110] X. Chen, C. Dong, J. Ji, J. Cao, and X. Li, "Image manipulation detection by multi-view multi-scale supervision," in *ICCV*, 2021. 4

[111] J. Johnson, A. Alahi, and L. Fei-Fei, "Perceptual losses for real-time style transfer and super-resolution," in *ECCV*, 2016. 4

[112] C. Shu, H. Wu, H. Zhou, J. Liu, Z. Hong, C. Ding, J. Han, J. Liu, E. Ding, and J. Wang, "Few-shot head swapping in the wild," in *CVPR*, 2022. 4

[113] Q. Wang, L. Liu, M. Hua, P. Zhu, W. Zuo, Q. Hu, H. Lu, and B. Cao, "Hs-diffusion: Semantic-mixing diffusion for head swapping," *arXiv*, 2023. 4

[114] Y. Han, J. Zhang, J. Zhu, X. Li, Y. Ge, W. Li, C. Wang, Y. Liu, X. Liu, and Y. Tai, "A generalist facex via learning unified facial representation," *arXiv*, 2023. 4, 6, 7, 23

[115] J. Zhang, C. Xu, J. Li, Y. Han, Y. Wang, Y. Tai, and Y. Liu, "Scsnet: An efficient paradigm for learning simultaneously image colorization and super-resolution," in *AAAI*, 2022. 4

[116] B. B. Moser, F. Raue, S. Frolov, S. Palacio, J. Hees, and A. Dengel, "Hitchhiker's guide to super-resolution: Introduction and recent advances," *TPAMI*, 2023. 4

[117] R. Natsume and Yatagawa, "Rsgan: face swapping and editing using face and hair representation in latent spaces," in *SIGGRAPH*, 2018. 4, 6, 23

[118] Q. Sun, A. Tewari, W. Xu, M. Fritz, C. Theobalt, and B. Schiele, "A hybrid model for identity obfuscation by face replacement," in *ECCV*, 2018. 4, 6, 23

[119] B. Fan, L. Wang, F. K. Soong, and L. Xie, "Photo-real talking head with deep bidirectional lstm," in *ICASSP*, 2015. 4, 8

[120] L. Chen, R. K. Maddox, Z. Duan, and C. Xu, "Hierarchical cross-modal talking face generation with dynamic pixel-wise loss," in *CVPR*, 2019. 4, 8, 9, 22, 24

[121] Y. Xu, B. Deng, J. Wang, Y. Jing, J. Pan, and S. He, "High-resolution face swapping via latent semantics disentanglement," in *CVPR*, 2022. 4, 6, 13, 23

[122] H. Huang, R. He, Z. Sun, and T. Tan, "Wavelet-srnet: A wavelet-based cnn for multi-scale face super resolution," in *ICCV*, 2017. 4, 12

[123] Z. Chen, J. Lin, T. Zhou, and F. Wu, "Sequential gating ensemble network for noise robust multiscale face restoration," *IEEE transactions on cybernetics*, 2019. 4, 12

[124] C. Chen, D. Gong, H. Wang, Z. Li, and K.-Y. K. Wong, "Learning spatial attention for face super-resolution," *TIP*, 2020. 4

[125] S. Ko and B.-R. Dai, "Multi-laplacian gan with edge enhancement for face super resolution," in *ICPR*, 2021. 4

[126] B. B. Moser, A. S. Shanbhag, F. Raue, S. Frolov, S. Palacio, and A. Dengel, "Diffusion models, image super-resolution and everything: A survey," in *AAAI*, 2024. 4

[127] Y. Shi, G. Li, Q. Cao, K. Wang, and L. Lin, "Face hallucination by attentive sequence optimization with reinforcement learning," *TPAMI*, 2019. 4

[128] K. Jiang, Z. Wang, P. Yi, G. Wang, K. Gu, and J. Jiang, "Atmfn: Adaptive-threshold-based multi-model fusion network for compressed face hallucination," *TMM*, 2019. 4

[129] A. Morales, G. Piella, and F. M. Sukno, "Survey on 3d face reconstruction from uncalibrated images," *Computer Science Review*, 2021. 4

[130] S. Sharma and V. Kumar, "3d face reconstruction in deep learning era: A survey," *ACME*, 2022. 4

[131] F. Maninchedda, M. R. Oswald, and M. Pollefeys, "Fast 3d reconstruction of faces with glasses," in *CVPR*, 2017. 5

[132] J. Lin, Y. Yuan, T. Shao, and K. Zhou, "Towards high-fidelity 3d face reconstruction from in-the-wild images using graph convolutional networks," in *CVPR*, 2020. 5

[133] M. Feng, S. Z. Gilani, Y. Wang, and A. Mian, "3d face reconstruction from light field images: A model-free approach," in *ECCV*, 2018. 5

[134] S. Tulsiani, T. Zhou, A. A. Efros, and J. Malik, "Multi-view supervision for single-view reconstruction via differentiable ray consistency," in *CVPR*, 2017. 5

[135] Y. Xing, R. Tewari, and P. Mendonca, "A self-supervised bootstrap method for single-image 3d face reconstruction," in *WACV*, 2019. 5

[136] I. Kemelmacher-Shlizerman and R. Basri, "3d face reconstruction from a single image using a single reference face shape," *TPAMI*, 2010. 5

[137] L. Jiang, J. Zhang, B. Deng, H. Li, and L. Liu, "3d face reconstruction with geometry details from a single image," *TIP*, 2018. 5

[138] P. Dou, S. K. Shah, and I. A. Kakadiaris, "End-to-end 3d face reconstruction with deep neural networks," in *CVPR*, 2017. 5

[139] B. Chaudhuri, N. Vesdapunt, L. Shapiro, and B. Wang, "Personalized face modeling for improved face reconstruction and motion retargeting," in *ECCV*, 2020. 5

[140] X. Zhang, D. Zhai, T. Li, Y. Zhou, and Y. Lin, "Image inpainting based on deep learning: A review," *Information Fusion*, 2023. 5

[141] A. B. Yildirim, H. Pehlivan, B. B. Bilecen, and A. Dundar, "Diverse inpainting and editing with gan inversion," in *ICCV*, 2023. 5

[142] M. Zhou, X. Liu, T. Yi, Z. Bai, and P. Zhang, "A superior image inpainting scheme using transformer-based self-supervised attention gan model," *Expert Systems with Applications*, 2023. 5

[143] J. Xu, S. Motamed, P. Vaddamanu, C. H. Wu, C. Haene, J.-C. Bazin, and F. De la Torre, "Personalized face inpainting with diffusion models by parallel visual attention," in *WACV*, 2024. 5

[144] P. Yang, S. Zhou, Q. Tao, and C. C. Loy, "Pgdiff: Guiding diffusion models for versatile face restoration via partial guidance," in *NeurIPS*, 2024. 5

[145] W.-Y. Yu, L.-M. Po, R. C. Cheung, Y. Zhao, Y. Xue, and K. Li, "Bidirectionally deformable motion modulation for video-based human pose transfer," in *ICCV*, 2023. 5

[146] X. Zhou, M. Yin, X. Chen, L. Sun, C. Gao, and Q. Li, "Cross attention based style distribution for controllable person image synthesis," in *ECCV*, 2022. 5, 12

[147] J. Zhao and H. Zhang, "Thin-plate spline motion model for image animation," in *CVPR*, 2022. 5, 12

[148] Y. Wang, X. Ma, X. Chen, A. Dantcheva, B. Dai, and Y. Qiao, "Leo: Generative latent image animator for human video synthesis," *arXiv*, 2023. 5, 9, 12

[149] T. Wang, L. Li, K. Lin, C.-C. Lin, Z. Yang, H. Zhang, Z. Liu, and L. Wang, "Disco: Disentangled control for referring human dance generation in real world," in *CVPR*, 2024. 5

[150] Z. Xu, J. Zhang, J. H. Liew, H. Yan, J.-W. Liu, C. Zhang, J. Feng, and M. Z. Shou, "Magicanimate: Temporally consistent human image animation using diffusion model," in *CVPR*, 2024. 5

[151] S. Yang, L. Jiang, Z. Liu, and C. C. Loy, "Vtoonify: Controllable high-resolution portrait video style transfer," *ACM TOG*, 2022. 5

[152] X. Peng, J. Zhu, B. Jiang, Y. Tai, D. Luo, J. Zhang, W. Lin, T. Jin, C. Wang, and R. Ji, "Portraitbooth: A versatile portrait model for fast identity-preserved personalization," in *CVPR*, 2024. 5

[153] Q. Cai, M. Ma, C. Wang, and H. Li, "Image neural style transfer: A review," *Computers and Electrical Engineering*, 2023. 5

[154] J. C. Pérez, T. Nguyen-Phuoc, C. Cao, A. Sanakoyeu, T. Simon, P. Arbeláez, B. Ghanem, A. Thabet, and A. Pumarola, "Styleavatar: Stylizing animatable head avatars," in *WACV*, 2024. 5

[155] J. Feng and P. Singhal, "3d face style transfer with a hybrid solution of nerf and mesh rasterization," in *WACV*, 2024. 5

[156] R. Abdal, H.-Y. Lee, P. Zhu, M. Chai, A. Siarohin, P. Wonka, and S. Tulyakov, "3davatargan: Bridging domains for personalized editable avatars," in *CVPR*, 2023. 5, 12

[157] S. Xu, L. Li, L. Shen, Y. Men, and Z. Lian, "Your3demoji: Creating personalized emojis via one-shot 3d-aware cartoon avatar synthesis," in *SIGGRAPH*, 2022. 5, 12

[158] Y. Jiang, L. Jiang, S. Yang, and C. C. Loy, "Scenimefy: Learning to craft anime scene via semi-supervised image-to-image translation," in *ICCV*, 2023. 5, 12

[159] J. Liu, H. Huang, C. Jin, and R. He, "Portrait diffusion: Training-free face stylization with chain-of-painting," *arXiv*, 2023. 5, 12

[160] J. Hur, J. Choi, G. Han, D.-J. Lee, and J. Kim, "Expanding expressiveness of diffusion models with limited data via self-distillation based fine-tuning," in *WACV*, 2024. 5, 12

[161] W. Jiang, S. Liu, C. Gao, J. Cao, R. He, J. Feng, and S. Yan, "Psgan: Pose and expression robust spatial-aware gan for customizable makeup transfer," in *CVPR*, 2020. 5, 12

[162] M. Li, W. Yu, Q. Liu, Z. Li, R. Li, B. Zhong, and S. Zhang, "Hybrid transformers with attention-guided spatial embeddings for makeup transfer and removal," *TCSVT*, 2023. 5, 12

[163] H. Chang, J. Lu, F. Yu, and A. Finkelstein, "Pairedcyclegan: Asymmetric style transfer for applying and removing makeup," in *CVPR*, 2018. 5, 12

[164] Q. Gu, G. Wang, M. T. Chiu, Y.-W. Tai, and C.-K. Tang, "Ladn: Local adversarial disentangling network for facial makeup and de-makeup," in *ICCV*, 2019. 5, 12

[165] S. Liu, W. Jiang, C. Gao, R. He, J. Feng, B. Li, and S. Yan, "Psgan++: robust detail-preserving makeup transfer and removal," *TPAMI*, 2021. 5, 12

[166] X. Zhong, X. Huang, Z. Wu, G. Lin, and Q. Wu, "Sara: Controllable makeup transfer with spatial alignment and region-adaptive normalization," *arXiv*, 2023. 5, 12

[167] C. Yang, W. He, Y. Xu, and Y. Gao, "Elegant: Exquisite and locally editable gan for makeup transfer," in *ECCV*, 2022. 5, 12

[168] Q. Yan, C. Guo, J. Zhao, Y. Dai, C. C. Loy, and C. Li, "Beautyrec: Robust, efficient, and component-specific makeup transfer," in *CVPR*, 2023. 5, 13

[169] Z. Sun, Y. Chen, and S. Xiong, "Ssat ++: A semantic-aware and versatile makeup transfer network with local color consistency constraint," *TNNLS*, 2023. **5**, 12

[170] M. Hao, G. Gu, H. Fu, C. Liu, and D. Cui, "Cumtgan: An instance-level controllable u-net gan for facial makeup transfer," *Knowledge-Based Systems*, 2022. **5**, 12

[171] S. Han, C. Lin, C. Shen, Q. Wang, and X. Guan, "Interpreting adversarial examples in deep learning: A review," *CSUR*, 2023. **5**

[172] C. Yuan, X. Liu, and Z. Zhang, "The current status and progress of adversarial examples attacks," in *CISCE*, 2021. **5**

[173] V. Blanz, K. Scherbaum, T. Vetter, and H.-P. Seidel, "Exchanging faces in images," in *Eurographics*, 2004. **5**, 6, 23

[174] D. Bitouk, N. Kumar, S. Dhillon, P. Bellumeur, and S. K. Nayar, "Face swapping: automatically replacing faces in photographs," in *SIGGRAPH*, 2008. **5**, 6, 23

[175] K. Dale, K. Sunkavalli, M. K. Johnson, D. Vlasic, W. Matusik, and H. Pfister, "Video face replacement," in *SIGGRAPH*, 2011. **5**, 6, 23

[176] Y. Lin, S. Wang, Q. Lin, and F. Tang, "Face swapping under large pose variations: A 3d model based approach," in *ICME*, 2012. **6**, 23

[177] J. Zhu, L. Van Gool, and S. C. Hoi, "Unsupervised face alignment by robust nonrigid mapping," in *ICCV*, 2009. **6**, 23

[178] Y. Nirkin, I. Masi, A. T. Tuan, T. Hassner, and G. Medioni, "On face segmentation, face swapping, and face perception," in *FG*, 2018. **5**, 6, 23

[179] X. P. Burgos-Artizzu, P. Perona, and P. Dollár, "Robust face landmark estimation under occlusion," in *ICCV*, 2013. **6**, 23

[180] Y. Nirkin, Y. Keller, and T. Hassner, "Fsgan: Subject agnostic face swapping and reenactment," in *ICCV*, 2019. **6**, 7, 23

[181] B. Maze, J. Adams, J. A. Duncan, N. Kalka, T. Miller, C. Otto, A. K. Jain, W. T. Niggel, J. Anderson, J. Cheney *et al.*, "Tarpa janus benchmark-c: Face dataset and protocol," in *ICB*, 2018. **6**, 23

[182] L. Li, J. Bao, H. Yang, D. Chen, and F. Wen, "Faceshifter: Towards high fidelity and occlusion aware face swapping," *CVPR*, 2020. **6**, 7, 11, 13, 23, 25

[183] B. Zhu, H. Fang, Y. Sui, and L. Li, "Deepfakes for medical video de-identification: Privacy protection and diagnostic information preservation," in *AAAI*, 2020. **6**, 23

[184] R. Chen, X. Chen, B. Ni, and Y. Ge, "Simswap: An efficient framework for high fidelity face swapping," in *ACM MM*, 2020. **6**, 13, 23

[185] Y. Zhu, Q. Li, J. Wang, C.-Z. Xu, and Z. Sun, "One shot face swapping on megapixels," in *CVPR*, 2021. **6**, 23

[186] J. Li, Z. Li, J. Cao, X. Song, and R. He, "Faceinpainter: High fidelity face adaptation to heterogeneous domains," in *CVPR*, 2021. **6**, 13, 23

[187] Y. Nirkin, Y. Keller, and T. Hassner, "Fsganv2: Improved subject agnostic face swapping and reenactment," *TPAMI*, 2022. **6**, 23

[188] J. Kim, J. Lee, and B.-T. Zhang, "Smooth-swap: a simple enhancement for face-swapping with smoothness," in *CVPR*, 2022. **6**, 7, 23

[189] H. Zeng, W. Zhang, C. Fan, T. Lv, S. Wang, Z. Zhang, B. Ma, L. Li, Y. Ding, and X. Yu, "Flowface: Semantic flow-guided shape-aware face swapping," in *AAAI*, 2023. **6**, 13, 23

[190] Y. Zhu, W. Zhao, Y. Tang, Y. Rao, J. Zhou, and J. Lu, "Stableswap: Stable face swapping in a shared and controllable latent space," *TMM*, 2024. **6**, 23

[191] K. Kim, Y. Kim, S. Cho, J. Seo, J. Nam, K. Lee, S. Kim, and K. Lee, "Diffface: Diffusion-based face swapping with facial guidance," *arXiv*, 2022. **6**, 7, 23

[192] W. Zhao, Y. Rao, W. Shi, Z. Liu, J. Zhou, and J. Lu, "Diffswap: High-fidelity and controllable face swapping via 3d-aware masked diffusion," in *CVPR*, 2023. **6**, 7, 13, 23

[193] K. Cui, R. Wu, F. Zhan, and S. Lu, "Face transformer: Towards high fidelity and accurate face swapping," in *CVPR*, 2023. **6**, 7, 23

[194] W. Cao, T. Wang, A. Dong, and M. Shu, "Transfs: Face swapping using transformer," in *FG*, 2023. **6**, 7, 23

[195] T. Wang, Z. Li, R. Liu, Y. Wang, and L. Nie, "An efficient attribute-preserving framework for face swapping," *TMM*, 2024. **6**, 23

[196] K. Sunkavalli, M. K. Johnson, W. Matusik, and H. Pfister, "Multi-scale image harmonization," *ACM TOG*, 2010. **5**, 23

[197] H. Guo, D. Niu, X. Kong, and X. Zhao, "Face replacement based on 2d dense mapping," in *ICIGP*, 2019. **6**

[198] J. R. A. Moniz, C. Beckham, S. Rajotte, S. Honari, and C. Pal, "Unsupervised depth estimation, 3d face rotation and replacement," in *NeurIPS*, 2018. **6**

[199] K. Liu, I. Perov, D. Gao, N. Chervoniy, W. Zhou, and W. Zhang, "Deepfacelab: Integrated, flexible and extensible face-swapping framework," *PR*, 2023. **6**, 23

[200] J. Bao, D. Chen, F. Wen, H. Li, and G. Hua, "Towards open-set identity preserving face synthesis," in *CVPR*, 2018. **6**, 23

[201] C. Xu, J. Zhang, Y. Han, G. Tian, X. Zeng, Y. Tai, Y. Wang, C. Wang, and Y. Liu, "Designing one unified framework for high-fidelity face reenactment and swapping," in *ECCV*, 2022. **6**

[202] D. Jiang, D. Song, R. Tong, and M. Tang, "Styleipsb: Identity-preserving semantic basis of stylegan for high fidelity face swapping," in *CVPR*, 2023. **6**, 13

[203] Y. Wang, X. Chen, J. Zhu, W. Chu, Y. Tai, C. Wang, J. Li, Y. Wu, F. Huang, and R. Ji, "Hififace: 3d shape and semantic prior guided high fidelity face swapping," in *IJCAI*, 2021. **6**, 13, 23

[204] X. Ren, X. Chen, P. Yao, H.-Y. Shum, and B. Wang, "Reinforced disentanglement for face swapping without skip connection," in *ICCV*, 2023. **6**, 13, 23

[205] Y. Zhang, H. Zeng, B. Ma, W. Zhang, Z. Zhang, Y. Ding, T. Lv, and C. Fan, "Flowface++: Explicit semantic flow-supervised end-to-end face swapping," *arXiv*, 2023. **6**, 13

[206] Z. Liu, M. Li, Y. Zhang, C. Wang, Q. Zhang, J. Wang, and Y. Nie, "Fine-grained face swapping via regional gan inversion," in *CVPR*, 2023. **7**, 23

[207] F. Rosberg, E. E. Aksoy, F. Alonso-Fernandez, and C. Englund, "Facedancer: pose-and occlusion-aware high fidelity face swapping," in *WACV*, 2023. **7**

[208] G. Gao, H. Huang, C. Fu, Z. Li, and R. He, "Information bottleneck disentanglement for identity swapping," in *CVPR*, 2021. **7**

[209] Z. Xu, H. Zhou, Z. Hong, Z. Liu, J. Liu, Z. Guo, J. Han, J. Liu, E. Ding, and J. Wang, "Styleswap: Style-based generator empowers robust face swapping," in *ECCV*, 2022. **7**, 13, 23

[210] F. Liu, L. Yu, H. Xie, C. Liu, Z. Ding, Q. Yang, and Y. Zhang, "High fidelity face swapping via semantics disentanglement and structure enhancement," in *ACM MM*, 2023. **7**, 23

[211] S.-M. Yoo, T.-M. Choi, J.-W. Choi, and J.-H. Kim, "Fastswap: A lightweight one-stage framework for real-time face swapping," in *WACV*, 2023. **7**

[212] I. Korshunova, W. Shi, J. Dambre, and L. Theis, "Fast face-swap using convolutional neural networks," in *ICCV*, 2017. **7**, 23

[213] G. Yuan, M. Li, Y. Zhang, and H. Zheng, "Reliableswap: Boosting general face swapping via reliable supervision," *arXiv*, 2023. **7**, 23

[214] J. Thies, M. Zollhofer, M. Stamminger, C. Theobalt, and M. Nießner, "Face2face: Real-time face capture and reenactment of rgb videos," in *CVPR*, 2016. **7**, 8

[215] H. Kim, P. Garrido, A. Tewari, W. Xu, J. Thies, M. Niessner, P. Perez, C. Richardt, M. Zollhöfer, and C. Theobalt, "Deep video portraits," *ACM TOG*, 2018. **7**, 8

[216] H. Kim, M. Elgharib, M. Zollhöfer, H.-P. Seidel, T. Beeler, C. Richardt, and C. Theobalt, "Neural style-preserving visual dubbing," *ACM TOG*, 2019. **7**, 8

[217] M. C. Doukas, S. Zafeiriou, and V. Sharmanska, "Headgan: One-shot neural head synthesis and editing," in *ICCV*, 2021. **8**

[218] K. Yang, K. Chen, D. Guo, S.-H. Zhang, Y.-C. Guo, and W. Zhang, "Face2face ρ : Real-time high-resolution one-shot face reenactment," in *ECCV*, 2022. **7**, 8

[219] Y. Gao, Y. Zhou, J. Wang, X. Li, X. Ming, and Y. Lu, "High-fidelity and freely controllable talking head video generation," in *CVPR*, 2023. **7**, 8, 13

[220] O. Wiles, A. Koepke, and A. Zisserman, "X2face: A network for controlling face generation using images, audio, and pose codes," in *ECCV*, 2018. **7**, 8

[221] E. Zakharov, A. Shysheya, E. Burkov, and V. Lempitsky, "Few-shot adversarial learning of realistic neural talking head models," in *CVPR*, 2019. **7**, 8

[222] J. Zhang, X. Zeng, M. Wang, Y. Pan, L. Liu, Y. Liu, Y. Ding, and Fan, "Freenet: Multi-identity face reenactment," in *CVPR*, 2020. **7**, 8

[223] E. Zakharov, A. Ivakhnenko, A. Shysheya, and V. Lempitsky, "Fast bi-layer neural synthesis of one-shot realistic head avatars," in *ECCV*, 2020. **7**, 8

[224] S. Ha, M. Kersner, B. Kim, S. Seo, and D. Kim, "Marionette: Few-shot face reenactment preserving identity of unseen targets," in *AAAI*, 2020. **7**, 8, 22

[225] M. C. Doukas, E. Ververas, V. Sharmanska, and S. Zafeiriou, "Free-headgan: Neural talking head synthesis with explicit gaze control," *TPAMI*, 2023. **7**, 8, 13, 22

[226] P. Kellnhofer, A. Recasens, S. Stent, W. Matusik, and A. Torralba, "Gaze360: Physically unconstrained gaze estimation in the wild," in *ICCV*, 2019. [8](#), [13](#)

[227] X. Zhang, Y. Sugano, M. Fritz, and A. Bulling, "Appearance-based gaze estimation in the wild," in *CVPR*, 2015. [8](#), [13](#)

[228] B. Zhang, C. Qi, P. Zhang, B. Zhang, H. Wu, D. Chen, Q. Chen, Y. Wang, and F. Wen, "Metaportrait: Identity-preserving talking head generation with fast personalized adaptation," in *CVPR*, 2023. [7](#), [8](#)

[229] S. Yang, W. Wang, Y. Lan, X. Fan, B. Peng, L. Yang, and J. Dong, "Learning dense correspondence for nerf-based face reenactment," in *AAAI*, 2024. [7](#), [8](#)

[230] W. Li, L. Zhang, D. Wang, B. Zhao, Z. Wang, M. Chen, B. Zhang, Z. Wang, L. Bo, and X. Li, "One-shot high-fidelity talking-head synthesis with deformable neural radiance field," in *CVPR*, 2023. [7](#), [8](#), [13](#), [22](#)

[231] S. Bounareli, C. Tzepelis, V. Argyriou, I. Patras, and G. Tzimiropoulos, "Stylemask: Disentangling the style space of stylegan2 for neural face reenactment," in *FG*, 2023. [7](#), [8](#)

[232] S. Bounareli, C. Tzepelis, V. Argyriou, and I. Patras, "One-shot neural face reenactment via finding directions in gan's latent space," *IJCV*, 2024. [7](#), [8](#)

[233] S. Tripathy, J. Kannala, and E. Rahtu, "Icface: Interpretable and controllable face reenactment using gans," in *WACV*, 2020. [8](#)

[234] T. Oorloff and Y. Yacoob, "Robust one-shot face video re-enactment using hybrid latent spaces of stylegan2," in *ICCV*, 2023. [8](#)

[235] H. Xue, J. Ling, A. Tang, L. Song, R. Xie, and W. Zhang, "High-fidelity face reenactment via identity-matched correspondence learning," *TOMM*, 2023. [8](#)

[236] X. Zeng, Y. Pan, M. Wang, J. Zhang, and Y. Liu, "Realistic face reenactment via self-supervised disentangling of identity and pose," in *AAAI*, 2020. [8](#)

[237] H. Zhang, Y. Ren, Y. Chen, G. Li, and T. H. Li, "Exploiting multiple guidance from 3dmm for face reenactment," in *AAAI/W*, 2023. [8](#)

[238] Y. Zhou, X. Han, E. Shechtman, J. Echevarria, E. Kalogerakis, and D. Li, "Makeltalk: speaker-aware talking-head animation," *ACM TOG*, 2020. [8](#), [9](#), [24](#)

[239] X. Ji, H. Zhou, K. Wang, W. Wu, C. C. Loy, X. Cao, and F. Xu, "Audio-driven emotional video portraits," in *CVPR*, 2021. [9](#), [24](#)

[240] Y. Gan, Z. Yang, X. Yue, L. Sun, and Y. Yang, "Efficient emotional adaptation for audio-driven talking-head generation," in *ICCV*, 2023. [8](#), [9](#), [13](#), [24](#)

[241] W. Zhang, X. Cun, X. Wang, Y. Zhang, X. Shen, Y. Guo, Y. Shan, and F. Wang, "Sadtalker: Learning realistic 3d motion coefficients for stylized audio-driven single image talking face animation," in *CVPR*, 2023. [8](#), [9](#), [24](#)

[242] Z. Peng, H. Wu, Z. Song, H. Xu, X. Zhu, J. He, H. Liu, and Z. Fan, "Emotalk: Speech-driven emotional disentanglement for 3d face animation," in *ICCV*, 2023. [9](#), [24](#)

[243] J. Wang, X. Qian, M. Zhang, R. T. Tan, and H. Li, "Seeing what you said: Talking face generation guided by a lip reading expert," in *CVPR*, 2023. [8](#), [9](#), [24](#)

[244] H. Zhou, Y. Sun, W. Wu, C. C. Loy, X. Wang, and Z. Liu, "Pose-controllable talking face generation by implicitly modularized audio-visual representation," in *CVPR*, 2021. [8](#), [9](#), [13](#), [24](#)

[245] B. Liang, Y. Pan, Z. Guo, H. Zhou, Z. Hong, X. Han, J. Han, J. Liu, E. Ding, and J. Wang, "Expressive talking head generation with granular audio-visual control," in *CVPR*, 2022. [8](#), [9](#), [13](#), [24](#)

[246] L. Yu, H. Xie, and Y. Zhang, "Multimodal learning for temporally coherent talking face generation with articulator synergy," *TMM*, 2021. [9](#), [24](#)

[247] C. Xu, J. Zhu, J. Zhang, Y. Han, W. Chu, Y. Tai, C. Wang, Z. Xie, and Y. Liu, "High-fidelity generalized emotional talking face generation with multi-modal emotion space learning," in *CVPR*, 2023. [8](#), [9](#), [13](#), [24](#)

[248] J. Wang, K. Zhao, S. Zhang, Y. Zhang, Y. Shen, D. Zhao, and J. Zhou, "Lipformer: High-fidelity and generalizable talking face generation with a pre-learned facial codebook," in *CVPR*, 2023. [8](#), [9](#), [24](#)

[249] S. Wang, Y. Ma, Y. Ding, Z. Hu, C. Fan, T. Lv, Z. Deng, and X. Yu, "Styletalk++: A unified framework for controlling the speaking styles of talking heads," *TPAMI*, 2024. [9](#), [24](#)

[250] C. Du, Q. Chen, T. He, X. Tan, X. Chen, K. Yu, S. Zhao, and J. Bian, "Dae-talker: High fidelity speech-driven talking face generation with diffusion autoencoder," in *ACM MM*, 2023. [9](#), [24](#)

[251] Z. Yu, Z. Yin, D. Zhou, D. Wang, F. Wong, and B. Wang, "Talking head generation with probabilistic audio-to-visual diffusion priors," in *ICCV*, 2023. [9](#), [24](#)

[252] M. Stypulkowski, K. Vougioukas, S. He, M. Zieba, S. Petridis, and M. Pantic, "Diffused heads: Diffusion models beat gans on talking-face generation," in *WACV*, 2024. [9](#), [24](#)

[253] B. Zhang, X. Zhang, N. Cheng, J. Yu, J. Xiao, and J. Wang, "Emotalker: Emotionally editable talking face generation via diffusion model," in *ICASSP*, 2024. [9](#), [24](#)

[254] Y. Guo, K. Chen, S. Liang, Y.-J. Liu, H. Bao, and J. Zhang, "Ad-nerf: Audio driven neural radiance fields for talking head synthesis," in *ICCV*, 2021. [9](#), [24](#)

[255] S. Shen, W. Li, Z. Zhu, Y. Duan, J. Zhou, and J. Lu, "Learning dynamic facial radiance fields for few-shot talking head synthesis," in *ECCV*, 2022. [8](#), [9](#), [24](#)

[256] D. Li, K. Zhao, W. Wang, B. Peng, Y. Zhang, J. Dong, and T. Tan, "Ae-nerf: Audio enhanced neural radiance field for few shot talking head synthesis," in *AAAI*, 2024. [9](#), [24](#)

[257] Z. Peng, W. Hu, Y. Shi, X. Zhu, X. Zhang, H. Zhao, J. He, H. Liu, and Z. Fan, "Sync talk: The devil is in the synchronization for talking head synthesis," in *CVPR'24*, 2024. [9](#), [24](#)

[258] Z. Ye, T. Zhong, Y. Ren, J. Yang, W. Li, J. Huang, Z. Jiang, J. He, R. Huang, J. Liu *et al.*, "Real3d-portrait: One-shot realistic 3d talking portrait synthesis," in *ICLR*, 2024. [9](#), [24](#)

[259] J. Zhang, L. Liu, Z. Xue, and Y. Liu, "Apb2face: Audio-guided face reenactment with auxiliary pose and blink signals," in *ICASSP*, 2020. [8](#)

[260] X. Wu, P. Hu, Y. Wu, X. Lyu, Y.-P. Cao, Y. Shan, W. Yang, Z. Sun, and X. Qi, "Speech2lip: High-fidelity speech to lip generation by learning from a short video," in *ICCV*, 2023. [8](#)

[261] D. Lee, C. Kim, S. Yu, J. Yoo, and G.-M. Park, "Radio: Reference-agnostic dubbing video synthesis," in *WACV*, 2024. [8](#), [24](#)

[262] H. Fu, Z. Wang, K. Gong, K. Wang, T. Chen, H. Li, H. Zeng, and W. Kang, "Mimic: Speaking style disentanglement for speech-driven 3d facial animation," in *AAAI*, 2024. [8](#)

[263] Z. Sheng, L. Nie, M. Zhang, X. Chang, and Y. Yan, "Stochastic latent talking face generation towards emotional expressions and head poses," *TCSV*, 2023. [8](#), [13](#)

[264] S. Tan, B. Ji, and Y. Pan, "Emmn: Emotional motion memory network for audio-driven emotional talking face generation," in *ICCV*, 2023. [8](#), [13](#)

[265] S. Zhai, M. Liu, Y. Li, Z. Gao, L. Zhu, and L. Nie, "Talking face generation with audio-deduced emotional landmarks," *TNNLS*, 2023. [8](#), [13](#)

[266] S. Gururani, A. Mallya, T.-C. Wang, R. Valle, and M.-Y. Liu, "Space: Speech-driven portrait animation with controllable expression," in *ICCV*, 2023. [8](#), [13](#), [24](#)

[267] Y. Ma, S. Wang, Y. Ding, B. Ma, T. Lv, C. Fan, Z. Hu, Z. Deng, and X. Yu, "Talkclip: Talking head generation with text-guided expressive speaking styles," *arXiv*, 2023. [8](#), [13](#)

[268] W. Zhong, C. Fang, Y. Cai, P. Wei, G. Zhao, L. Lin, and G. Li, "Identity-preserving talking face generation with landmark and appearance priors," in *CVPR*, 2023. [8](#), [24](#)

[269] C. Xu, S. Zhu, J. Zhu, T. Huang, J. Zhang, Y. Tai, and Y. Liu, "Multimodal-driven talking face generation via a unified diffusion-based generator," *CoRR*, 2023. [9](#)

[270] J. Karras, A. Holynski, T.-C. Wang, and I. Kemelmacher-Shlizerman, "Dreampose: Fashion image-to-video synthesis via stable diffusion," in *ICCV*, 2023. [9](#)

[271] E. R. Chan, C. Z. Lin, M. A. Chan, K. Nagano, B. Pan, S. De Mello, O. Gallo, L. J. Guibas, J. Tremblay, S. Khamis *et al.*, "Efficient geometry-aware 3d generative adversarial networks," in *CVPR*, 2022. [9](#), [12](#)

[272] B. Kerbl, G. Kopanas, T. Leimkühler, and G. Drettakis, "3d gaussian splatting for real-time radiance field rendering," *ACM TOG*, 2023. [9](#)

[273] S. Zhou, T. Xiao, Y. Yang, D. Feng, Q. He, and W. He, "Genegan: Learning object transfiguration and attribute subspace from unpaired data," in *BMVC*, 2017. [9](#), [10](#), [24](#)

[274] Y. Jo and J. Park, "Sc-fegan: Face editing generative adversarial network with user's sketch and color," in *ICCV*, 2019. [10](#), [24](#)

[275] Y. Shen, J. Gu, X. Tang, and B. Zhou, "Interpreting the latent space of gans for semantic face editing," in *CVPR*, 2020. [9](#), [10](#), [24](#)

[276] X. Yao, A. Newson, Y. Gousseau, and P. Hellier, "A latent transformer for disentangled face editing in images and videos," in *ICCV*, 2021. [9](#), [10](#), [24](#)

[277] Y. Gao, F. Wei, J. Bao, S. Gu, D. Chen, F. Wen, and Z. Lian, "High-fidelity and arbitrary face editing," in *CVPR*, 2021. [9](#), [10](#), [13](#), [24](#)

[278] K. Preechakul, N. Chatthee, S. Wizadwongsu, and S. Suwajanakorn, "Diffusion autoencoders: Toward a meaningful and decodable representation," in *CVPR*, 2022. [10](#), [14](#), [24](#)

[279] J. Sun, X. Wang, Y. Zhang, X. Li, Q. Zhang, Y. Liu, and J. Wang, "Fenerf: Face editing in neural radiance fields," in *CVPR*, 2022. [10](#), [13](#), [24](#)

[280] Z. Huang, K. C. Chan, Y. Jiang, and Z. Liu, "Collaborative diffusion for multi-modal face generation and editing," in *CVPR*, 2023. [10](#), [24](#)

[281] S. Ozkan, M. Ozay, and T. Robinson, "Conceptual and hierarchical latent space decomposition for face editing," in *ICCV*, 2023. [10](#), [24](#)

[282] P. Zhou, L. Xie, B. Ni, and Q. Tian, "Cips-3d++: End-to-end real-time high-resolution 3d-aware gans for gan inversion and stylization," *TPAMI*, 2023. [10](#), [24](#)

[283] C. Yu, G. Lu, Y. Zeng, J. Sun, X. Liang, H. Li, Z. Xu, S. Xu, W. Zhang, and H. Xu, "Towards high-fidelity text-guided 3d face generation and manipulation using only images," in *ICCV*, 2023. [10](#), [13](#), [24](#)

[284] Y. Dalva, S. F. Altindis, and A. Dundar, "Vecgan: Image-to-image translation with interpretable latent directions," in *ECCV*, 2022. [10](#), [24](#)

[285] Z. Ding, X. Zhang, Z. Xia, L. Jebe, Z. Tu, and X. Zhang, "Diffusionrig: Learning personalized priors for facial appearance editing," in *CVPR*, 2023. [10](#), [24](#)

[286] G. Kim, H. Shim, H. Kim, Y. Choi, J. Kim, and E. Yang, "Diffusion video autoencoders: Toward temporally consistent face video editing via disentangled video encoding," in *CVPR*, 2023. [10](#), [14](#), [24](#)

[287] W. L. Wenmin Huang and X. C. Jiwu Huang, "Sdgan: Disentangling semantic manipulation for facial attribute editing," in *AAAI*, 2024. [10](#), [24](#)

[288] H. Zhang, T. DAI, Y. Xu, Y.-W. Tai, and C.-K. Tang, "Facednerf: Semantics-driven face reconstruction, prompt editing and relighting with diffusion models," in *NIPS*, 2024. [10](#), [24](#)

[289] W. Shen and R. Liu, "Learning residual images for face attribute manipulation," in *CVPR*, 2017. [9](#), [24](#)

[290] Y. Xu, Y. Yin, L. Jiang, Q. Wu, C. Zheng, C. C. Loy, B. Dai, and W. Wu, "Transendor: Transformer-based dual-space gan for highly controllable facial editing," in *CVPR*, 2022. [9](#), [24](#)

[291] X. Hou, X. Zhang, H. Liang, L. Shen, Z. Lai, and J. Wan, "Guidedstyle: Attribute knowledge guided style manipulation for semantic face editing," *Neural Networks*, 2022. [9](#), [13](#), [24](#)

[292] X. Hou, X. Zhang, Y. Li, and L. Shen, "Textface: Text-to-style mapping based face generation and manipulation," *TMM*, 2022. [10](#), [13](#)

[293] S. Aneja, J. Thies, A. Dai, and M. Nießner, "Clipface: Text-guided editing of textured 3d morphable models," in *SIGGRAPH*, 2023. [10](#), [24](#)

[294] L. Li, J. Bao, T. Zhang, H. Yang, D. Chen, F. Wen, and B. Guo, "Face x-ray for more general face forgery detection," in *CVPR*, 2020. [11](#), [14](#), [25](#)

[295] Y. Nirkin, L. Wolf, Y. Keller, and T. Hassner, "Deepfake detection based on discrepancies between faces and their context," *TPAMI*, 2021. [10](#), [11](#), [25](#)

[296] K. Shiohara and T. Yamasaki, "Detecting deepfakes with self-blended images," in *CVPR*, 2022. [10](#), [11](#), [14](#), [25](#)

[297] J. Cao, C. Ma, T. Yao, S. Chen, S. Ding, and X. Yang, "End-to-end reconstruction-classification learning for face forgery detection," in *CVPR*, 2022. [10](#), [11](#), [14](#), [25](#)

[298] T. Wang and K. P. Chow, "Noise based deepfake detection via multi-head relative-interaction," in *AAAI*, 2023. [10](#), [11](#), [25](#)

[299] Z. Ba, Q. Liu, Z. Liu, S. Wu, F. Lin, L. Lu, and K. Ren, "Exposing the deception: Uncovering more forgery clues for deepfake detection," in *AAAI*, 2024. [10](#), [11](#), [25](#)

[300] Y. Zheng, J. Bao, D. Chen, M. Zeng, and F. Wen, "Exploring temporal coherence for more general video face forgery detection," in *ICCV*, 2021. [11](#), [14](#), [25](#)

[301] A. Haliassos, K. Vougioukas, S. Petridis, and M. Pantic, "Lips don't lie: A generalisable and robust approach to face forgery detection," in *CVPR*, 2021. [11](#), [13](#), [14](#), [25](#)

[302] Z. Gu, Y. Chen, T. Yao, S. Ding, J. Li, and L. Ma, "Delving into the local: Dynamic inconsistency learning for deepfake video detection," in *AAAI*, 2022. [11](#), [25](#)

[303] J. Choi, T. Kim, Y. Jeong, S. Baek, and J. Choi, "Exploiting style latent flows for generalizing deepfake detection video detection," in *CVPR*, 2024. [11](#), [25](#)

[304] Y. Xu, J. Liang, L. Sheng, and X.-Y. Zhang, "Towards generalizable deepfake video detection with thumbnail layout and graph reasoning," *IJCV*, 2024. [11](#), [25](#)

[305] C. Miao, Z. Tan, Q. Chu, N. Yu, and G. Guo, "Hierarchical frequency-assisted interactive networks for face manipulation detection," *TIFS*, 2022. [11](#), [25](#)

[306] Z. Guo, Z. Jia, L. Wang, D. Wang, G. Yang, and N. Kasabov, "Constructing new backbone networks via space-frequency interactive convolution for deepfake detection," *TIFS*, 2023. [11](#), [25](#)

[307] C. Tan, Y. Zhao, S. Wei, G. Gu, P. Liu, and Y. Wei, "Frequency-aware deepfake detection: Improving generalizability through frequency space domain learning," in *AAAI*, 2024. [11](#), [25](#)

[308] H. Dang, F. Liu, J. Stehouwer, X. Liu, and A. K. Jain, "On the detection of digital face manipulation," in *CVPR*, 2020. [11](#), [12](#), [25](#)

[309] T. Zhao, X. Xu, M. Xu, H. Ding, Y. Xiong, and W. Xia, "Learning self-consistency for deepfake detection," in *ICCV*, 2021. [11](#), [12](#), [13](#), [14](#), [25](#)

[310] J. Hu, X. Liao, J. Liang, W. Zhou, and Z. Qin, "Finfer: Frame inference-based deepfake detection for high-visual-quality videos," in *AAAI*, 2022. [11](#), [12](#), [25](#)

[311] X. Guo, X. Liu, Z. Ren, S. Grosz, I. Masi, and X. Liu, "Hierarchical fine-grained image forgery detection and localization," in *CVPR*, 2023. [11](#), [12](#), [25](#)

[312] S. McCloskey and M. Albright, "Detecting gan-generated imagery using saturation cues," in *ICIP*, 2019. [10](#), [25](#)

[313] H. Zhao, W. Zhou, D. Chen, T. Wei, W. Zhang, and N. Yu, "Multi-attentional deepfake detection," in *CVPR*, 2021. [10](#), [14](#), [25](#)

[314] L. Chai, D. Bau, S.-N. Lim, and P. Isola, "What makes fake images detectable? understanding properties that generalize," in *ECCV*, 2020. [10](#), [25](#)

[315] Z. Liu, X. Qi, and P. H. Torr, "Global texture enhancement for fake face detection in the wild," in *CVPR*, 2020. [10](#), [25](#)

[316] H. H. Nguyen, J. Yamagishi, and I. Echizen, "Capsule-forensics: Using capsule networks to detect forged images and videos," in *ICASSP*, 2019. [10](#)

[317] D. Cozzolino, A. Pianese, M. Nießner, and L. Verdoliva, "Audio-visual person-of-interest deepfake detection," in *CVPR*, 2023. [11](#)

[318] C. Feng, Z. Chen, and A. Owens, "Self-supervised video forensics by audio-visual anomaly detection," in *CVPR*, 2023. [11](#)

[319] S. Agarwal and H. Farid, "Detecting deep-fake videos from aural and oral dynamics," in *CVPR*, 2021. [11](#)

[320] J. Frank, T. Eisenhofer, L. Schönherr, A. Fischer, D. Kolossa, and T. Holz, "Leveraging frequency analysis for deep fake image recognition," in *ICML*, 2020. [11](#), [25](#)

[321] I. Masi, A. Killekar, R. M. MAscarenhas, S. P. Gurudatt, and W. AbdAlmageed, "Two-branch recurrent network for isolating deepfakes in videos," in *ECCV*, 2020. [11](#), [14](#)

[322] C.-C. Hsu, C.-Y. Lee, and Y.-X. Zhuang, "Learning to detect fake face images in the wild," in *IS3C*, 2018. [12](#), [25](#)

[323] N. Yu, L. S. Davis, and M. Fritz, "Attributing fake images to gans: Learning and analyzing gan fingerprints," in *ICCV*, 2019. [12](#), [25](#)

[324] R. Wang, F. Juefei-Xu, L. Ma, X. Xie, Y. Huang, J. Wang, and Y. Liu, "Fakespotter: a simple yet robust baseline for spotting ai-synthesized fake faces," in *IJCAI*, 2021. [12](#)

[325] Y. Guo, C. Zhen, and P. Yan, "Controllable guide-space for generalizable face forgery detection," in *ICCV*, 2023. [12](#), [13](#), [14](#)

[326] X. Hu, P. Ma, Z. Mai, S. Peng, Z. Yang, and L. Wang, "Face hallucination from low quality images using definition-scalable inference," *PR*, 2019. [12](#)

[327] T. Lu, J. Wang, J. Jiang, and Y. Zhang, "Global-local fusion network for face super-resolution," *Neurocomputing*, 2020. [12](#)

[328] W. Zhang, Y. Liu, C. Dong, and Y. Qiao, "Ranksrgan: Generative adversarial networks with ranker for image super-resolution," in *ICCV*, 2019. [12](#)

[329] Y. Pan, J. Tang, and T. Tjahjadi, "Lpsrgan: Generative adversarial networks for super-resolution of license plate image," *Neurocomputing*, 2024. [12](#)

[330] B. Lei, K. Yu, M. Feng, M. Cui, and X. Xie, "Diffusiongan3d: Boosting text-guided 3d generation and domain adaption by combining 3d gans and diffusion priors," *arXiv*, 2023. [12](#)

[331] R. Jain, K. K. Singh, M. Hemani, J. Lu, M. Sarkar, D. Ceylan, and B. Krishnamurthy, "Vgflow: Visibility guided flow network for human reposing," in *CVPR*, 2023. [12](#)

[332] L. Hu, X. Gao, P. Zhang, K. Sun, B. Zhang, and L. Bo, "Animate anyone: Consistent and controllable image-to-video synthesis for character animation," *arXiv*, 2023. [12](#)

[333] D. Guo and T. Sim, "Digital face makeup by example," in *CVPR*, 2009. [12](#)

[334] C. Li, K. Zhou, and S. Lin, "Simulating makeup through physics-based manipulation of intrinsic image layers," in *CVPR*, 2015. [12](#)

[335] H.-J. Chen, K.-M. Hui, S.-Y. Wang, L.-W. Tsao, H.-H. Shuai, and W.-H. Cheng, "Beautyglow: On-demand makeup transfer framework with reversible generative network," in *CVPR*, 2019. [12](#)

[336] Z. Sun, Y. Chen, and S. Xiong, "Ssat: A symmetric semantic-aware transformer network for makeup transfer and removal," in *AAAI*, 2022. [12](#)

[337] M. Agarwal, R. Mukhopadhyay, V. P. Namboodiri, and C. Jawahar, "Audio-visual face reenactment," in *WACV*, 2023. [13](#)

[338] Y. Deng, J. Yang, S. Xu, D. Chen, Y. Jia, and X. Tong, "Accurate 3d face reconstruction with weakly-supervised learning: From single image to image set," in *CVPR*, 2019. [22](#)

[339] J. Deng, J. Guo, N. Xue, and S. Zafeiriou, "Arcface: Additive angular margin loss for deep face recognition," in *CVPR*, 2019. [22](#)

[340] S. Mosaddegh, L. Simon, and F. Jurie, "Photorealistic face de-identification by aggregating donors' face components," in *ACCV*, 2015. [23](#)

[341] R. Gross, I. Matthews, J. Cohn, T. Kanade, and S. Baker, "Multi-pie," *IVC*, 2010. [23](#)

[342] S. Milborrow, J. Morkel, and F. Nicolls, "The muct landmarked face database," *PRASA*, 2010. [23](#)

[343] Y. Guo, L. Zhang, Y. Hu, X. He, and J. Gao, "Ms-celeb-1m: A dataset and benchmark for large-scale face recognition," in *ECCV*, 2016. [23, 24](#)

[344] N. Zhang, M. Paluri, Y. Taigman, R. Fergus, and L. Bourdev, "Beyond frontal faces: Improving person recognition using multiple cues," in *CVPR*, 2015. [23](#)

[345] "Deepglint," <http://trillionpairs.deepglint.com>, 2023. [23](#)

[346] Y. Li, C. Ma, Y. Yan, W. Zhu, and X. Yang, "3d-aware face swapping," in *CVPR*, 2023. [23](#)

[347] C.-H. Lee, Z. Liu, L. Wu, and P. Luo, "Maskgan: Towards diverse and interactive facial image manipulation," in *CVPR*, 2020. [23](#)

[348] M. Cooke, J. Barker, S. Cunningham, and X. Shao, "An audio-visual corpus for speech perception and automatic speech recognition," *JASA*, 2006. [24](#)

[349] C. Richie, S. Warburton, and M. Carter, "Audiovisual database of spoken american english," *LDC*, 2009. [24](#)

[350] H. Zhou, Y. Liu, Z. Liu, P. Luo, and X. Wang, "Talking face generation by adversarially disentangled audio-visual representation," in *AAAI*, 2019. [24](#)

[351] S. R. Livingstone and F. A. Russo, "The ryerson audio-visual database of emotional speech and song (ravdess): A dynamic, multimodal set of facial and vocal expressions in north american english," *PLoS one*, 2018. [24](#)

[352] C. Zhang, C. Wang, J. Zhang, H. Xu, G. Song, Y. Xie, L. Luo, Y. Tian, X. Guo, and J. Feng, "Dream-talk: Diffusion-based realistic emotional audio-driven method for single image talking face generation," *arXiv*, 2023. [24](#)

[353] Z. He, W. Zuo, M. Kan, S. Shan, and X. Chen, "Attgan: Facial attribute editing by only changing what you want," *TIP*, 2019. [24](#)

[354] "Media forensics challenge," <https://www.nist.gov/itl/iad/mig/media-forensicschallenge-2018>, 2018. [25](#)

[355] Y. Li and S. Lyu, "Exposing deepfake videos by detecting face warping artifacts," in *CVPRW*, 2018. [25](#)

[356] T. Zhou, W. Wang, Z. Liang, and J. Shen, "Face forensics in the wild," in *CVPR*, 2021. [25](#)

[357] A. Ciamarra, R. Caldelli, F. Becattini, L. Seidenari, and A. Del Bimbo, "Deepfake detection by exploiting surface anomalies: the surface approach," in *WACV*, 2024. [25](#)

[358] J. Tian, P. Chen, C. Yu, X. Fu, X. Wang, J. Dai, and J. Han, "Learning to discover forgery cues for face forgery detection," *TIFS*, 2024. [25](#)

[359] F. Song, X. Tan, X. Liu, and S. Chen, "Eyes closeness detection from still images with multi-scale histograms of principal oriented gradients," *PR*, 2014. [25](#)

[360] H. Guan, M. Kozak, E. Robertson, Y. Lee, A. N. Yates, A. Delgado, D. Zhou, T. Kheykhah, J. Smith, and J. Fiscus, "Mfc datasets: Large-scale benchmark datasets for media forensic challenge evaluation," in *WACV*, 2019. [25](#)

[361] C. Peng, Z. Miao, D. Liu, N. Wang, R. Hu, and X. Gao, "Where deepfakes gaze at? spatial-temporal gaze inconsistency analysis for video face forgery detection," *TIFS*, 2024. [25](#)

[362] F. Yu, A. Seff, Y. Zhang, S. Song, T. Funkhouser, and J. Xiao, "Lsun: Construction of a large-scale image dataset using deep learning with humans in the loop," *arXiv*, 2015. [25](#)

[363] "Casia image tampering detection evaluation database 2010," <http://forensics.idealtest.org>, 2010. [25](#)

[364] Y. Zhai, T. Luan, D. Doermann, and J. Yuan, "Towards generic image manipulation detection with weakly-supervised self-consistency learning," in *ICCV*, 2023. [25](#)

[365] J. Dong, W. Wang, and T. Tan, "Casia image tampering detection evaluation database," in *ChinaSIP*, 2013. [25](#)

[366] Y.-F. Hsu and S.-F. Chang, "Detecting image splicing using geometry invariants and camera characteristics consistency," in *ICME*, 2006. [25](#)

[367] B. Wen, Y. Zhu, R. Subramanian, T.-T. Ng, X. Shen, and S. Winkler, "Coverage—a novel database for copy-move forgery detection," in *ICIP*, 2016. [25](#)

[368] A. Novozamsky, B. Mahdian, and S. Saic, "Imd2020: A large-scale annotated dataset tailored for detecting manipulated images," in *WACV*, 2020. [25](#)

APPENDIX

A. METRICS

- **Face Swapping.** The most commonly used objective evaluation metrics for face swapping include ID Ret, Expression Error, Pose Error, and FID. ID Ret is calculated by a pre-trained face recognition model [102], measuring the Euclidean distance between the generated face and the source face. A higher ID Ret indicates better preservation of identity information. Expression and pose errors quantify the differences in expression and pose between the generated face and the source face. These metrics are evaluated using a pose estimator [104] and a 3D facial model [338], extracting expression and pose vectors for the generated and source faces. Lower values for expression error and pose error indicate higher facial expression and pose similarity between the swapped face and the source face. FID [100] is used to assess image quality, with lower FID values indicating that the generated images closely resemble authentic facial images in appearance.

- **Face Reenactment and Talking Face Generation.** Face reenactment commonly uses consistent evaluation metrics, including CSIM, SSIM [98], PSNR, LPIPS [99], LMD [105], and FID. CSIM describes the cosine similarity between the generated and source faces, calculated by ArcFace [339], with higher values indicating better performance. SSIM, PSNR, LPIPS, and FID are used to measure the quality of synthesized images. SSIM measures the structural similarity between two images, with higher values indicating a closer resemblance to natural images. PSNR quantifies the ratio between a signal's maximum possible power and noise's power, indicating higher quality for higher values. LPIPS assesses reconstruction fidelity using a pre-trained AlexNet [52] to extract feature maps for similarity score computation. As mentioned earlier, FID is used to evaluate image quality. LMD assesses the accuracy of lip shape in generated images or videos, with lower values indicating better model performance.

Expanding upon face reenactment metrics, talking face generation incorporates additional metrics, including M/F-LMD, Sync, LSE-C, and LSE-D. The LSE-C and LSE-D are usually used to measure lip synchronization effectiveness [106]. The landmark distances on the mouth (M-LMD) [120] and the confidence score of SyncNet (Sync) measure synchronization between the generated lip motion and the input audio. F-LMD computes the difference in the average distance of all landmarks between predictions and ground truth (GT) as a measure to assess the generated expression. In addition, there are some meaningful metrics, such as LSE-C and LSE-D for measuring lip synchronization effectiveness [106], AVD [230] for evaluating identity preservation performance, AUCON [224] for assessing facial pose and expression jointly, and AGD [225] for evaluating eye gaze changes. These newly proposed evaluation metrics enrich the performance assessment system by targeting various aspects of the model's performance.

- **Facial Attribute Editing.** The standard evaluation metrics used in face attribute manipulation are FID, LPIPS [99], KID [101], PSNR and SSIM. KID is one of the image quality assessment metrics commonly used in face editing work and

other generative modeling tasks to quantify the difference in distribution between the generated image and the actual image, with lower KID values indicating better model performance. Some text-guide work will also use the CLIP Score to measure the consistency between the output image and the text, calculated as the cosine similarity between the normalized image and the text embedding. Higher values of CLIP Score indicate better consistency of the generated image with the corresponding text sentence.

B. SUPPLEMENTARY TABLES

This section supplements some of the table content in the main text, further expanding the number of models introduced. Tab. 16 supplements Tab. 2 in the main text, Tab. 17 supplements Tab. 4 in the main text, Tab. 18 supplements Tab. 5 and Tab. 19 supplements Tab. 6 in the main text.

TABLE 16: Overview of representative face swapping methods. Notations: ❶ Self-build, ❷ CelebA-HQ, ❸ FFHQ, ❹ VGGFace2, ❺ VGGFace, ❻ CelebV, ❼ CelebA, ❼ VoxCeleb2, ❽ LFW, ❾ KoDF. Abbreviations: SIGGRAPH (SIG.), GANs (G.), VAEs (V.), Diffusion (D.), Split-up and Integration (SI.).

	Method	Venue	Dataset	Categorize	Limitation	Highlight
Traditional Graphics	Blanz <i>et al.</i> [173]	EG'04	❶	3DMM	Manual intervention, unnatural output.	Early face-swapping efforts simplified manual interaction steps.
	Bitouk <i>et al.</i> [174]	SIG'08	❶	SI.	Manual intervention, attribute loss.	A three-phase implementation framework with the help of a pre-constructed face database to match faces that are similar to the source face in terms of posture and lighting.
	Sunkavalli <i>et al.</i> [196]	TOG'10	❶	SI.	Poor generalizability, frequent artifacts.	Early work on face exchange was realized using image processing methods such as smooth histogram matching technique.
	Dale <i>et al.</i> [175]	SIG'11	❶	3DMM	Poor generalizability and output quality.	Early work on face exchange, proposed an improved Poisson mixing approach to achieve face swapping in video through frame-by-frame face replacement.
	Lin <i>et al.</i> [176]	ICME'12	[177]	3DMM	Poor generalizability, frequent artifacts.	An attempt to construct a personalized 3D head model to solve the artifact problem occurring in face swapping in large poses.
	Mosadegh <i>et al.</i> [340]	ACCV'14	[341] [342]	SI.	Poor generalizability and output quality.	A diverse form of face swapping where facial components can be targeted for replacement.
	Nirkin <i>et al.</i> [178]	FG'18	[179]	SI.	Poor generalization ability and resolution.	Transfer of expressions and poses by building some 3D variable models and training facial segmentation networks to maintain target facial occlusion.
	IPGAN [200]	CVPR'18	[343]	G.+V.	Poor output image quality, frequent artifacts.	Using two encoders to encode facial identity and attribute information separately for facial information decoupling and swapping.
	RSGAN [117]	SIG'18	❼	G.+V.	Loss of lighting information.	Using two independent VAE modules to represent the latent spaces of the face and hair regions, respectively, with the replacement of identity information in the latent space implemented.
	Sun <i>et al.</i> [118]	ECCV'18	[344]	G.+3DMM	Poor ability to preserve face feature attributes.	Implementing in two stages: the first stage involves replacing the identity information of the face region, while the second stage achieves complete facial rendering.
Generative Adversarial Network Based	FSGAN [180]	ICCV'19	[181]	G.	Poor ability to preserve face feature attributes.	Two novel loss functions are introduced to refine the stitching in the face fusion phase following the face swapping process.
	FaceShifter [182]	CVPR'20	❶❷❸❹	G.	Poor ability to preserve face feature attributes.	The first stage AEI-Net improves the output image quality level and the second HEAR-Net is targeted to focus on abnormal regions for image recovery.
	Zhu <i>et al.</i> [183]	AAAI'20	❶	G.+V.	Inability to process facial contour information.	First show of the applicability of deepfake to keypoint invariant de-identification work.
	DeepFaceLab [199]	PR'20	❶	G.+V.	Poor output image resolution.	A mature and complete framework for face swapping.
	SimSwap [184]	MM'20	❶❷	G.+V.	Poor ability to preserve face feature attributes.	ID injection modules and weak feature matching loss functions are proposed in an effort to find a balance between identity information replacement and attribute information retention.
	MegaFS [185]	CVPR'21	❶❷❸	G.	Poor ability to preserve face feature attributes.	The first method allows for face swapping on images with a resolution of one million pixels.
	FaceInpainter [186]	CVPR'21	❶❷❸❹	G.+3DMM	Poor representation of image details.	A two-stage framework innovatively implements heterogeneous domains face swapping.
	HifiFace [203]	IJCAI'21	❶ [345]	G.+3DMM	Uses a large number of parameters.	A 3D shape-aware identity extractor is proposed to achieve better retention of attribute information such as facial shape.
	FSGANv2 [187]	TPAMI'22	❶ [181]	G.	Unable to process posture differences effectively.	An extension of the FSGAN method that combines Poisson optimization with perceptual loss enhances the output image facial details.
	StyleSwap [209]	ECCV'22	❶❷❸	G.	Unable to process posture differences effectively.	Proposing an exchange-guided ID reversal strategy to enhance the performance of attribute information replacement during face exchange.
Diffusion	RAFSwap [11]	CVPR'22	❷	G.	Unable to process posture differences effectively.	Local facial region awareness branch with global source feature adaptation (SFA) branch is proposed to better achieve the preservation of target image attribute information.
	FSLSD [121]	CVPR'22	❶❷	G.	Poor ability to preserve face feature attributes.	Potential semantic de-entanglement is realized to obtain facial structural attributes and appearance attributes in a hierarchical manner.
	Kim <i>et al.</i> [188]	CVPR'22	❷❸	G.	Unable to process posture differences effectively.	A identity embedder is proposed to enhance the training speed under supervised.
	3DSwap [346]	CVPR'23	❷❸	G.+3DMM	Unable to process posture differences effectively.	A 3d-aware approach to the face-swapping task, de-entangling identity and attribute features in latent space in an effort to achieve identity replacement and attribute feature retention.
	FALCO [10]	CVPR'23	❷❸	G.	Poor ability to handle facial occlusion.	Oriented with privacy-preserving applications, the method directly employs the latent space of pre-trained GANs to achieve the identity of anonymized images while preserving facial attributes.
	E4S [206]	CVPR'23	❷ [347]	G.	Poor ability to preserve face feature attributes.	This work enables the global or local exchange of facial features. A new local GAN inversion method is proposed, aiming at decoupling identity information from attribute information.
	WSC-Swap [204]	ICCV'23	❶❷❸❹	G.+3DMM	Poor resolution of the output image.	Two mutually independent encoders are proposed to encode attribute information outside the face region and semantic-level non-identical facial attributes inside the face region.
	BlendFace [13]	ICCV'23	❶❷❸❹	G.	Unable to handle occlusion and extreme lighting.	The identity features obtained from the de-entanglement are fed to the generator as an identity loss function, which guides the generator to generate an image to fit the source image identity information.
	FlowFace [189]	AAAI'23	❶❷❸❹	G.+3DMM	Altered target image lighting details.	It consists of face reshaping network and face exchange network, which better solves the influence of the difference between source and target face contours on the face exchange work.
	S2Swap [210]	MM'23	❷❸❹	G.+3D	Poor ability to preserve face feature attributes.	Achieving high-fidelity face swapping through semantic disentanglement and structural enhancement.
Other	StableSwap [190]	TMM'24	❷❸	G.+3D	Unable to handle extreme skin color differences.	Utilizing a multi-stage identity injection mechanism effectively combines facial features from both the source and target to produce high-fidelity face swapping.
	DiffFace [191]	arXiv'22	❸❹	D.	Facial lighting attributes are altered.	Claims to be the first diffusion model-based face exchange framework.
	DiffSwap [192]	CVPR'23	❸❹	D.	Poor ability to handle facial occlusion.	Reenvisioning face swapping as conditional inpainting to harness the power of the diffusion model.
	FaceX [114]	arXiv'23	❸❹❺	D.	Unable to handle extreme skin color differences.	A novel facial all-rounder model capable of performing various facial tasks.
	Liu <i>et al.</i> [9]	arXiv'24	❶❷❸	D.	Poor ability to preserve face feature attributes.	Conditional diffusion model introduces balanced identity and expression encoders components, achieving a balance between identity replacement and attribute preservation during the generation process.
Other	Fast Face-swap [212]	ICCV'17	❼	Other	Unable to handle occlusion and extreme lighting.	Facial swapping is implemented based on the style transfer, and a new loss function is designed to obtain more realistic output results.
	Cui <i>et al.</i> [193]	CVPR'23	❷❸	Other	Altered target image lighting details.	Introducing a multiscale transformer network focusing on high-quality semantically aware correspondences between source and target faces.
	TransFS [194]	FG'23	❷❸❹	Other	Unable to process posture differences effectively.	The identity generator is designed to reconstruct high-resolution images of specific identities, and an attention mechanism is utilized to enhance the retention of identity information.
	ReliableSwap [213]	arXiv'23	❶❷❸❹	Other	Poor ability to preserve face feature attributes.	Constructing a supervisor called the "cyclic triplet" enhances model's identity preservation capability.
	Wang <i>et al.</i> [195]	TMM'24	❷❸	Other	Poor ability to handle facial occlusion.	A Global Residual Attribute-Preserving Encoder was proposed, and a network flow considering the facial landmarks of the target face was introduced, achieving high-quality face swapping.

TABLE 17: An overview table of talking face generation methods. Corresponding labels for the commonly used datasets are ① LFW, ② VoxCeleb2, ③ MEAD, ④ Self-build, ⑤ LRS2, ⑥ HDTF, ⑦ LRS3, ⑧ CREMA-D, ⑨ VoxCeleb, ⑩ FFHQ.

	Method	Year	Dataset	Limitation	Highlight
Audio / Text - Driven	Chen <i>et al.</i> [105]	ECCV'18	① [348] [349]	Poor resolution, inability to control pose and emotional.	Proposed a novel generator network and a comprehensive model with four complementary losses, as well as a new audio-visual related loss function to guide video generation.
	Zhou <i>et al.</i> [350]	AAAI'19	① [343]	Inability to control pose and emotional variations.	Generate high-quality talking face videos by disentangling audio-visual representations.
	Chen <i>et al.</i> [120]	CVPR'19	① [348]	Inability to control pose and emotional variations.	Proposed a cascaded approach, using facial landmarks as an intermediate high-level representation.
	Wav2Lip [106]	ICMR'20	①②⑦	Poor resolution, inability to control pose and emotional.	A new evaluation framework and a dataset for training mouth synchronization are proposed.
	MakeItTalk [238]	TOG'20	②	Unable to control pose and emotional variations well.	Separating content information and identity information from audio signals, combining LSTM and self-attention mechanism to enhance head movement coherence.
	Ji <i>et al.</i> [239]	CVPR'21	①③	Inability to control pose and emotional variations.	By breaking down the input audio sample into content and emotion embeddings, cross-reconstruction of emotional disentanglement creates facial landmarks with nuanced emotional content.
	SPACE [266]	ICCV'23	②③ [351]	Lack emotional and other latent attributes control	Constructed a novel facial intermediate representation, achieving control over head pose, blinking, and gaze direction.
	Gan <i>et al.</i> [240]	ICCV'23	①②③	Insufficient emotional output diversity.	Proposed a two-stage architecture, implementing speaker generation independent of emotion and embedding emotion information.
	SadTalker [241]	CVPR'23	②③	Lack emotional and other latent attributes control.	Based on the idea of 3DMM and conditional VAE, 3D coefficients controlling facial motion and expression are generated from audio to realize the reproduction of accurate face from audio.
	Zhong <i>et al.</i> [268]	CVPR'23	②⑦ [389]	Lack emotional and other latent attributes control.	A two-stage framework for step-by-step audio-to-face action generation is proposed.
Multimodal	TalkLip [243]	CVPR'23	①③	Inability to control pose and emotional variations.	Pre-trained lip-reading experts are employed to penalize incorrect lip-reading predictions in the synthesized videos.
	DR2 [19]	WACV'24	②	Lack emotional and other latent attributes control.	The model explored effective strategies for reducing the training workload.
	RADIO [261]	WACV'24	①②③	Lack emotional and other latent attributes control.	Introducing StyleGAN2 style modulation to adapt to human identity and utilizes ViT blocks to focus on facial attributes in the reference image.
	PC-AVS [244]	CVPR'21	①②	Lack emotional and other latent attributes control.	Introduction of pose-source video drive compensation to generate head motion in video.
	GC-AVT [245]	CVPR'22	②③	Poor resolution, unable to handle complex backgrounds.	In addition to the source image, a gesture source, an expression source, and audio are introduced to drive the talking head generation.
	Yu <i>et al.</i> [246]	TMM'22	④	Lack emotional and other latent attributes control.	Fusion of audio and text inputs for more accurate lip movement and chin posture prediction.
	Xu <i>et al.</i> [247]	CVPR'23	③	Insufficient control over the intensity of emotional output.	Embedding textual, visual, and auditory emotional modalities into a unified space.
	LipFormer [248]	CVPR'23	②③	Poor ability to preserve face feature attributes.	Propose retaining high-quality facial details obtained from pre-training in a codebook format and reproducing them by driving the encoded mapping relationship between audio and lip movements.
	Wang <i>et al.</i> [249]	TPAMI'24	②③⑥	Unable to delicately control emotions.	Using 3DMM as an intermediate variable to convey facial expressions and head movements, and introducing additional reference videos to extract the desired speaking style.
	DAE-Talker [250]	MM'23	④	High model complexity.	It replaces traditional manually crafted intermediate representations with data-driven latent representations obtained from a DAE.
Diffusion	Yu <i>et al.</i> [251]	ICCV'23	②③	Poor resolution, high model complexity.	Building a corresponding mapping between audio and non-lip representations and training using the diffusion model.
	DreamTalk [18]	arXiv'23	②③⑥	Mismatched emotion and semantics, occasional artifacts.	The denoising network, style-aware lip expert, and style predictor collaborate to make the model perform well in various speaking styles.
	DREAM-Talk [352]	arXiv'23	②③	High model complexity.	Proposed a two-stage approach to effectively capture subtle emotional nuances and ensure accurate lip synchronization.
	Stypulkowski [252]	WACV'24	①③	High model complexity, short video generation duration.	The model incorporates motion frame and audio embedding information to capture past movements and future expressions, with an emphasis on the mouth region through an additional lip sync loss.
	EmoTalker [253]	ICASSP'24	②③	High model complexity.	It achieves emotion-editable talking face generation based on a conditional diffusion model.
	AD-NeRF [254]	ICCV'21	④	Inadequate control of emotions and latent attributes.	The NeRF based approach achieves accurate reproduction of detailed facial components and generates the upper body region.
	DFRF [255]	ECCV'22	④	Lack of emotional and other latent attributes control.	Combining audio with 3D perceptual features and proposing an facial deformation module.
	EmoTalk [242]	ICCV'23	②③	Poor real-time performance and expression details.	An emotion-entangled encoder and emotion-guided decoder enable emotion injection, with outputs generated using Blendshape and FLAME model rendering.
	AE-NeRF [256]	AAAI'24	⑥	Lack emotional and other latent attributes control.	Facial modeling is divided into NeRF related to audio and unrelated to audio to enhance audio-visual lip synchronization and facial detail.
	SyncTalk [257]	CVPR'24	④	Lack controllable emotional intensity regulation.	The facial sync controller boosts component coordination, and a portrait generator corrects artifacts, enhancing video details.
3D-Model	Ye <i>et al.</i> [258]	ICLR'24	② [76]	Lack emotional control and occasional artifacts.	Facial and audio information is separately represented using tri-plane, followed by rendering. The generated results are further optimized based on the super-resolution network.

TABLE 18: Overview of representative facial attribute editing methods. Notations: ① FFHQ, ② CelebA, ③ CelebA-HQ, ④ CelebAMask-HQ, ⑤ VoxCeleb, ⑥ CelebAText-HQ, ⑦ LFW, ⑧ MM CelebA-HQ, ⑨ CARLA, ⑩ Multi-PIE. In addition, some abbreviations are used in the table: SIGGRAPH (SIG.), GANs (G.), Diffusion (D.), Transformer (T.).

Method	Venue	Categorize Dataset	Highlight
Shen <i>et al.</i> [289]	CVPR'17	G.	②⑦ Initial efforts in attribute editing concentrated on training distinct models for particular attributes, where the central concept was to comprehend the differences pre-manipulation and post-manipulation, depicted as residual images.
GeneGAN [273]	BMVC'17	G.	②⑩ In early attribute editing, separate models were trained for specific attributes. The key idea was to reassemble attribute vectors in the latent space, achieving successful editing.
SC-FEGAN [274]	ICCV'19	G.	③ Users can generate high-quality edited output images by freely sketching parts of the source image.
AttGAN [353]	TIP'19	G.	② Applying attribute classification constraints to generated images has validated the drawbacks of enforcing stringent attribute independence constraints in latent representations.
Shen <i>et al.</i> [275]	CVPR'20	G.	② Thoroughly investigated how to encode different semantics in the latent space and explored the disentanglement between various semantics to achieve precise control over facial attributes.
Yao <i>et al.</i> [276]	ICCV'21	G.+T.	③ By integrating explicit decoupling terms and identity-consistent terms into the loss function, the preservation of facial identity information is improved, resulting in high-quality face editing in videos.
HifaFace [277]	CVPR'21	G.	① Proposed a solution based on wavelet transform to address the issue of partial loss of attribute information when generating edited results due to "cyclic consistency" problems.
Preechakul <i>et al.</i> [278]	CVPR'22	D.	① When encoding images, it is divided into semantically meaningful parts and parts that represent the details of the image.
FENeRF [279]	CVPR'22	G.+NeRF	④ The introduction of semantic masks into the conditional radiance field enables finer image textures.
GuidedStyle [291]	NN'22	G.	① Generating faces after face editing is guided based on facial attribute classification. The introduction of a sparse attention mechanism enhances the manipulation of individual attribute styles.
FDNeRF [29]	SIG.'22	G.+NeRF	⑤ The introduction of the Conditional Feature Warping (CFW) module addresses the issue of temporal inconsistency caused by dynamic information in the process of face editing in videos.
AnyFace [20]	CVPR'22	G.	⑥⑧ Proposed a dual-branch framework for text-driven facial editing, with coordination achieved between the two branches through a Cross-Modal Distillation (CMD) module.
TransEditor [290]	CVPR'22	G.	③⑪ Emphasizing dual-space GAN interaction's importance, a transformer architecture is introduced for improved interaction.
Huang <i>et al.</i> [280]	CVPR'23	D.	④ Proposed the concept of assisted diffusion, integrating individual multimodalities to explore the complementarity between different modalities.
Ozkan <i>et al.</i> [281]	ICCV'23	G.	① The entangled attribute space is decomposed into conceptual and hierarchical latent spaces, and transformer network encoders are employed to modify information in the latent space.
CIPS-3D++ [282]	TPAMI'23	G.+NeRF	⑩⑪ Replaced the convolutional architecture with an MLP (Multi-Layer Perceptron) architecture to achieve faster rendering speeds.
ClipFace [293]	SIG.'23	G.+3DMM	① Learned texture generation from large-scale datasets, enhancing generator performance through generative adversarial training.
TG-3DFace [283]	ICCV'23	G.	⑩⑫ For different scenarios, two sets of text-to-face cross-modal alignment methods were designed with specific focuses.
VecGAN++ [284]	TPAMI'23	G.	③ Orthogonal constraint and disentanglement loss are used to decouple attribute vectors in the latent space.
DiffusionRig [285]	CVPR'23	D.	① 3DMM and diffusion model integration propose a two-stage method for learning personalized facial details.
Kim <i>et al.</i> [286]	CVPR'23	D.	⑥ Proposed a method for facial editing in videos based on the diffusion model.
SDGAN <i>et al.</i> [287]	AAAI'24	G.	③ SDGAN introduces a semantic separation generator and a semantic mask alignment strategy, achieving satisfactory preservation of irrelevant details and precise attribute manipulation.
FaceDNeRF [288]	NIPS'24	D.+NeRF	① Creating and editing facial NeRFs with single-view images, text prompts, and target lighting.

TABLE 19: Overview of representative forgery detection methods. Notations: ① FF++, ② DFDC, ③ Celeb-DF, ④ Deeperfornatics, ⑤ Self-build, ⑥ UADFV, ⑦ Celeb-HQ, ⑧ DFDCp, ⑨ FFHQ, ⑩ DFD.

	Method	Year	Train	Test	Highlight
Based on Space Domain	McCloskey <i>et al.</i> [312]	ICIP'19	[354]	⑦ [354]	GANs' exposure handling differs from real cameras, suggesting that image saturation can be used as a perspective for detecting forgeries.
	Li <i>et al.</i> [355]	CVPRW'19	⑤	⑥ [77]	It focuses on the unique artifacts generated when algorithms further distort the forged face to match the original face in the source video.
	Gram-Net [315]	CVPR'20	⑦⑨	⑦⑨	The method posits that genuine faces and fake faces exhibit inconsistencies in texture details.
	Face X-ray [294]	CVPR'20	①	①②③④	Focusing on boundary artifacts of face fusion for forgery detection.
	Chai <i>et al.</i> [314]	ECCV'20	①⑤⑦	①⑤⑨	It focuses on the inherent differences between images captured by a camera and manipulated images.
	Zhao <i>et al.</i> [313]	CVPR'21	①	①②③	A texture enhancement module, an attention generation module, and a bilinear attention pooling module are proposed to focus on texture details.
	Nirkin <i>et al.</i> [295]	TPAMI'21	①	①②③	Detecting swapped faces by comparing the facial region with its context (non-facial area).
	SBIs [296]	CVPR'22	①	②③④⑩ [356]	The belief that the more difficult to detect forged faces typically contain more generalized traces of forgery can encourage the model to learn a feature representation with greater generalization ability.
	RECCE [297]	CVPR'22	①	①②③ [92]	Reconstruction learning on real samples to learn common compressed representations of real facial images.
	LGrad [30]	CVPR'23	⑥	⑥	The gradient is utilized to present generalized artifacts that are fed into the classifier to determine the truth of the image.
Based on Time Domain	NoiseDF [298]	AAAI'23	①	①②③④	Focus on extracting noise traces and features from cropped faces and background squares of video image frames.
	Ciamarra <i>et al.</i> [357]	WACV'24	①	①	By analyzing the depicted surface features in an image, the inconsistency of the unambiguous environment represented by pixel values is exploited as a detection criterion.
	Ba <i>et al.</i> [299]	AAAI'24	①②③	①②③	Multiple non-overlapping local representations are extracted from the image for forgery detection. A local information loss function, based on information bottleneck theory, is proposed for constraint.
	Tian <i>et al.</i> [358]	TIFS'24	①②③⑥	①②③⑥	A weakly supervised model using a classification attention region module for forgery clue detection and a complementary learning module for enhanced clue learning is introduced.
	Liet <i>et al.</i> [91]	WIFS'18	⑥ [359]	[359]	Detecting the authenticity of a video by analyzing whether blinking occurs and the frequency of blinking.
	Yang <i>et al.</i> [94]	ICASSP'19	⑥ [360]	⑥ [360]	Focusing on the inconsistency in the head pose in videos by comparing the estimated head pose using all facial landmarks with the one estimated using only the landmarks in the central region.
	FTCN [300]	ICCV'21	①	①②③④ [182]	It is believed that most face video forgeries are generated frame by frame. As each altered face is independently generated, this inevitably leads to noticeable flickering and discontinuity.
	LipForensics [301]	CVPR'21	①	①②③	Concern about temporal inconsistency of mouth movements in videos.
	M2TR [108]	ICMR'22	①	①②③④	Capturing local inconsistencies at different scales for forgery detection using a multiscale transformer.
	Gu <i>et al.</i> [302]	AAAI'22	①	①②③ [92]	By densely sampling adjacent frames, the method pays attention to the inter-frame image inconsistency.
Frequency	Franket <i>et al.</i> [320]	CVPR'22	①	①②③④ [182]	Focus on the natural correspondence between faces and audio in video.
	Yang <i>et al.</i> [34]	TIFS'23	①②③	①②③	Treating DeepFake detection as a graph classification problem and focuses on the relationship information between facial regions to consider the relationship between local image features across different frames.
	AVoID-DF [39]	TIFS'23	②⑥	②⑥ [84]	Multimodal forgery detection using audiovisual inconsistency.
	Choi <i>et al.</i> [303]	CVPR'24	①③④	①③	Focus on the inconsistency of the style latent vectors between frames.
	Xu <i>et al.</i> [304]	IJCV'24	①②③④	①②③④	Forgery detection is conducted by converting video clips into thumbnails containing both spatial and temporal information.
	Peng <i>et al.</i> [361]	TIFS'24	①③⑥ [92]	①③⑥ [92]	Adopting the idea of physiological signal detection, focusing on the temporal and spatial gaze inconsistency in video face forgery detection.
	Frank <i>et al.</i> [320]	ICML'20	⑤	⑨ [69]	Severe artifacts in GAN-generated images can be easily identified in the frequency space, which stem from the upsampling steps used in GANs.
	F3-Net [36]	ECCV'20	①	①	A two-branch frequency perception framework with a cross-attention module is proposed.
	FDFL [37]	CVPR'21	①	①	Propose an adaptive frequency feature generation module to extract differential features from different frequency bands in a learnable manner.
	HFI-Net [305]	TIFS'22	①	②③④⑥ [77]	Notice that the forgery flaws used to distinguish between real and fake faces are concentrated in the mid- and high-frequency spectrum.
Data Driven	Guo <i>et al.</i> [306]	TIFS'23	①②	①②③	Designing a backbone network for Deepfake detection with space-frequency interaction convolution.
	Tan <i>et al.</i> [307]	AAAI'24	⑥	①⑥ [362]	A lightweight frequency-domain learning network is proposed to constrain classifier operation within the frequency domain.
	DeepFD [322]	IS3C'18	⑤ [69]	⑤	Introducing a contrastive loss enables the model to learn discriminative features from training images across multiple GANs.
	Yu <i>et al.</i> [323]	ICCV'19	[69] [362]	[69] [362]	Assuming that each GAN model generates images with a unique fingerprint, targeted forgery detection during training can be achieved.
	Dang <i>et al.</i> [308]	CVPR'20	⑤	③⑥	Utilizing attention mechanisms to handle the feature maps of the detection model.
	Zhao <i>et al.</i> [309]	ICCV'21	①	①②③④⑤⑩	Proposes pairwise self-consistent learning for training CNN to extract these source features and detect deep vacation images.
Human	Finfer [310]	AAAI'22	①	①③⑥ [92]	Finfer utilizes an autoregressive model, using the facial representation of the current frame to predict the facial representation of future frames.
	Huang <i>et al.</i> [109]	CVPR'23	①	①②③⑩ [182]	A new implicit identity-driven face exchange detection framework is proposed.
	Hi-Fi-Net [311]	CVPR'23	⑤	⑤ [363]	Converting image forgery detection and localization into a hierarchical fine-grained classification problem.
	Zhai <i>et al.</i> [364]	ICCV'23	[365]	[363] [366] [367] [368]	Weakly supervised image processing detection is proposed such that only binary image level labels (real or tampered) are required for training.